8 Monoclonal Antibodies: From Structure to Therapeutic Application

Rong Deng, C. Andrew Boswell, Wendy S. Putnam, Meina T. Tang, Amit Garg, Chunze Li, Shan Chung, and Sandhya Girish

INTRODUCTION

The exciting field of therapeutic monoclonal antibodies (MABs) had its origins when Köhler and Milstein presented their murine hybridoma technology in 1975 (Kohler and Milstein 1975). This technology provides a reproducible method for producing MABs with unique target selectivity in almost unlimited quantities. In 1984, both scientists received the Nobel Prize for their scientific breakthrough, and their work is viewed as a key milestone in the history of MABs as therapeutic modalities and their other applications. Although it took some time until the first therapeutic MAB received FDA approval in 1986 (Orthoclone OKT3, Chap. 25), MABs are now the standard of care in several disease areas. In particular, in oncology (Chap. 23), transplantation (Chap. 25), and inflammatory diseases (Chap. 26), patients now have novel life-changing treatment alternatives for diseases that had very limited or nonexistent medical treatment options before the emergence of MABs. Today, more than 75 MABs and MAB derivatives, including fusion proteins and MAB fragments, are available for a variety of indications (Table 8.1). The majority of approved biologic therapies are MABs, antibody-drug conjugates (ADCs), antibody fragments, and Fc fusion proteins. Technological evolutions have subsequently allowed much wider application of MABs thanks to the ability to generate mouse/human chimeric, humanized, and fully human MABs from antibodies (Abs) of pure murine origin. In particular, the reduction of the xenogenic portion of the MAB structure decreased the immunogenic potential of murine MABs, allowing their wider application. MABs are generally well-tolerated drugs because of their target selectivity, thus avoiding unnecessary exposure to, and consequently activity in, nontarget organs. This is particularly apparent in the field of oncology where MABs such as rituximab, trastuzumab, bevacizumab, cetuximab and immune-oncology MABs such as atezolizumab, pembrolizumab and nivolumab can offer a more favorable risk-benefit profile compared to common chemotherapeutic treatment regimens for some hematologic cancers and solid tumors.

The advent of MABs not only resulted in new drugs, but also triggered the development of an entirely new business model for drug research and development and the founding of hundreds of biotech companies focused on MAB development. Furthermore, the ability to selectively target disease-related molecules with MABs helped to launch a new era of targeted medicine and set new standards for successful drug research and development. The term translational medicine was coined to describe the use of biochemical, biological, and (patho)physiological understanding to find novel interventions to treat disease. During this process, biomarkers (e.g., genetic expression levels of marker genes, protein expression of target proteins, or molecular imaging) can be used to gain deeper understanding of the biological activities of drugs in a qualitative and, most importantly, quantitative sense, essentially encompassing the entire field of pharmacokinetics and pharmacodynamics (PK/PD). The application of these scientific methods, together with the principle of molecular-targeted medicine and the favorable PK and safety of MABs, may at least partly explain the higher success rates of biotechnologically derived products in reaching the market compared to chemically derived small molecule drugs.

This chapter addresses the following topics: Antibody structure and classes, currently approved MAB based therapeutics, mechanisms of action, clinical development and drug properties. In this sense, this

R. Deng · W. S. Putnam · M. T. Tang · A. Garg
C. Li · S. Girish (✉)
Clinical Pharmacology, Genentech Inc.,
South San Francisco, CA, USA
e-mail: sandhyag@gene.com

C. A. Boswell
Preclinical and Translational Pharmacokinetics,
Genentech Inc., South San Francisco, CA, USA

S. Chung
Bioanalytical Sciences, Genentech Inc.,
South San Francisco, CA, USA

D. J. A. Crommelin et al. (eds.), *Pharmaceutical Biotechnology*, https://doi.org/10.1007/978-3-030-00710-2_8

Name	Therapeutic area	Antibody/antibody derivatives		Target		PK				
		Type	Structure	Receptor/ antigen	Type	Behavior[b]	Elimination/ terminal half-life[c]	Clearance (CL)/ apparent CL	Volume of distribution (V and apparent V)[d]	Route/dosing highlights
Abciximab	Cardiovascular/ metabolism	Fragment	Chimeric Fab: +D31mVar-hIgG1	CD41	Cell-bound	Linear	0.29 days[e]	0.068 L/h/kg[f]	0.12 L/kg	IV bolus, mg/kg dose
Alirocumab	Cardiovascular/ metabolism	MAB	hIgG1	PCSK9	Soluble	Nonlinear	17–20 days	NR	Central Vd: 0.04–0.05 L/kg	SC injection, flat mg dose
Dulaglutide	Cardiovascular/ metabolism	Fusion protein	Disulfide-linked homo-dimer GLP-1 + modified hIgG4H (Fc)	GLP-1 R	Cell-bound	NR	5 days	0.75 mg dose: 0.111 L/h 1.5 mg dose: 0.107 L/h	0.75 mg dose: 19.2 L 1.5 mg dose: 17.4 L	SC injection, flat mg dose
Evolocumab	Cardiovascular/ metabolism	MAB	hIgG2	PCSK9	Soluble	Nonlinear	11–17 days (effective $t_{1/2}$)	12 mL/h after 420 mg IV	3.3 L after 420 mg IV	SC injection, flat mg dose
Idarucizumab	Cardiovascular/ metabolism	Fragment	Humanized IgG1 (Fab)	Dabigatran and its acyl-glucuronide metabolites	N/A	NR	Initial: 47 min; terminal:10.3 h	47.0 mL/min	8.9 L	IV infusion, flat gram dose
Antihemophilic factor (recombinant), Fc fusion protein	Hemophilia	Fusion protein	B-domain deleted human coagulation Factor VIII + hIgG1 Fc	NR	NR	NR	1–5 years: 12.7 h 6–11 years: 14.9 h 12–17 years: 16.4 h Adults: 19.7 h	1–5 years: 3.60 mL/h/kg 6–11 years: 2.78 mL/h/kg 12–17 years: 2.66 mL/h/kg Adults: 2.06 mL/h/kg	–5 years: 58.6 mL/kg 6–11 years: 52.1 mL/kg 12–17 years: 60.3 mL/kg Adults: 49.5 mL/kg	IV injection, individualized per label
Alprolix	Hemophilia	Fusion protein	Human coagulation Factor IX + hIgG1 (Fc)	N/A	N/A	NR	50 IU/kg: 86 h 100 IU/kg: 91 h	50 IU/kg dose: 3.3 mL/h/kg 100 IU/kg: 2.6 mL/h/kg	50 IU/kg: 327 mL/kg 100 IU/kg: 236 mL/kg	IV infusion, IU/kg dose
Emicizumab-kxwh	Hemophilia	MAB	Humanized bi-specific IgG4	Factor IXa and factor X	Soluble	Linear within dose range of 0.3–3.0 mg/kg	27.8 ± 8.1 days	CL/F: 0.24 L/day (apparent)	V/F: 11.4 L (apparent)	SC injection, mg/kg dose
Palivizumab	Infectious disease	MAB	Humanized IgG1	RSV F protein	Cell-bound	NR	20 days	NR	NR	IM injection, mg/kg dose
Bezlotoxumab	Infectious disease	MAB	hIgG1	*C. difficile* toxin B	Cell-bound	Linear	19 days	0.317 L/day	7.33 L	IV infusion, mg/kg dose
Obiltoxaximab[g]	Infectious disease	MAB	Chimeric: mVar-hIgG1 kappa	PA component *B. anthracis* toxin	Cell bound	Linear over 4–16 mg/kg dose range	15–23 days	NR	NR	IV infusion, mg/kg dose
Abatacept	Inflammation/ autoimmunity	Fusion protein	hCTLA-4 ECD + hFc (hinge)	CD80, CD86	Cell-bound	Linear	13.1 days[h]	0.22 mL/h/kg[h]	0.07 L/kg	IV infusion, mg/kg dose
Adalimumab	Inflammation/ autoimmunity	MAB	hIgG1	TNFα	Soluble, cell-bound	Linear	14.7–19.3 days[i]	9–12 mL/h[i]	5.1–5.75 L: *F* = 64%	SC injection, flat mg dose
Alefacept[j]	Inflammation/ autoimmunity	Fusion protein	LFA-3 + hIgG1 (Fc)	CD2	Cell-bound	Nonlinear	11.3 days	0.25 (mL/h/kg)	IV: 94 mL/kg IM: *F* = 63%	IV infusion, flat mg dose

Belimumab	Inflammation/ autoimmunity	MAB	hIgG1	BLyS	Soluble, cell-bound	Linear	19.4 days	215 mL/day	5.29 L	IV infusion mg/ kg dose
Benralizumab	Inflammation/ autoimmunity	MAB	Humanized IgG1	IL-5Rα	Cell-bound	Linear at 20–200 mg range	15 days	70 kg patient: 0.29 L/day	70 kg patient: 5.7 L; SC: F ≈ 58%	SC injection, flat mg dose
Brodalumab	Inflammation/ autoimmunity	MAB	hIgG2	hIL-17RA	Cell-bound	Nonlinear	NR	CL/F: 3.0 ± 3.5 L/ day (apparent CL)	Vz/F: 8.9 ± 9.4 L (apparent Vz)	SC injection, flat mg dose
Canakinumab	Inflammation/ Autoimmunity	MAB	hIgG1	IL-1β	Soluble	Linear	26 days	0.174 L/day	6.01 L, *F* = 70%	SC injection, flat mg dose
Certolizumab pegol	Inflammation/ autoimmunity	Fragment	Humanized IgG1 (Fab) conjugated with PEG2MAL40K	TNFα	Soluble, cell-bound	Linear	14 days	9.21–14.38 mL/h	6–8 L, *F* = 76–88%	SC injection, flat mg dose
Daclizumab HYP	Inflammation/ autoimmunity	MAB	Humanized IgG1	CD25	Cell-bound	Linear	22 days	CL: 0.24 L/day CL/F: 0.274 L/ day (apparent CL)	6.41 L	SC injection, flat mg dose
Dupilumab[k]	Inflammation/ autoimmunity	MAB	hIgG4	IL-4Rα (common subunit IL-4R and IL-13R complexes)	Cell-bound	Nonlinear	NR	0.126 L/day	4.8 ± 1.3 L	SC injection, flat mg dose with loading dose
Eculizumab	Inflammation/ autoimmunity	MAB	Humanized IgG2/4 kappa	complement protein C5	Soluble	Linear	8–14.8 days	22 mL/h	7.7 L	IV infusion, flat mg dose
Efalizumab[l]	Inflammation/ autoimmunity	MAB	Humanized IgG1	CD11a	Cell-bound, internalized	Nonlinear	N/A	6.6 mL/kg/day[m]	58 mL/kg SC, *F* = 50%	SC injection, mg/kg dose
Etanercept	Inflammation/ autoimmunity	Fusion protein	TNF receptor + hIgG1 (Fc)	TNFα	Soluble, cell-bound	Linear	4 days[n]	120 mL/h; CL/F: 160 mL/hr[n]	*F*: 58%; Vd: 6–11 L	SC injection, flat mg dose
Golimumab	Inflammation/ autoimmunity	MAB	hIgG1	TNFα	Soluble, cell-bound	Linear	2 weeks	4.9–6.7 mL/day/ kg	Vd = 58–126 mL/kg; F = 53%	SC injection, flat mg dose
Infliximab	Inflammation/ autoimmunity	MAB	Chimeric: mVar-hIgG1	TNFα	Soluble, cell-bound	Linear	7.7–9.5 days	9.8 mL/h[o]	NR	IV infusion, mg/ kg dose
Ixekizumab	Inflammation/ autoimmunity	MAB	Humanized IgG4	IL-17A	Soluble, membrane bound	Linear	13 days	0.39 L/day	7.11 L	SC injection, flat mg dose with loading dose
Mepolizumab	Inflammation/ autoimmunity	MAB	Humanized IgG1, kappa	IL-5	Soluble	Linear	20 days (range 16–22 days)	70 kg patient: 0.28 L/day	70 kg patient: Vc = 3.6 L	SC injection, flat mg dose
Natalizumab	Inflammation/ autoimmunity	MAB	Humanized IgG4 kappa	α4 integrins	Cell-bound	NR	11 days	16 mL/h	NR	IV infusion, flat mg dose
Ocrelizumab	Inflammation/ autoimmunity	MAB	Humanized IgG1, glycosylated	CD20	Cell-bound	Nonlinear, linear over 400–2000 mg dose range	26 days	CL linear: 0.17 L/ day	Vc 2.78 L, Vp 2.68 L	IV infusion, flat mg dose

Table 8.1 ■ Therapeutic biologics (monoclonal antibodies, antibody fragments, fusion proteins and antibody-drug conjugates)[a]

Name	Therapeutic area	Antibody/antibody derivatives		Target		PK				
		Type	Structure	Receptor/ antigen	Type	Behavior[b]	Elimination/ terminal half-life[c]	Clearance (CL)/ apparent CL	Volume of distribution (V and apparent V)[d]	Route/dosing highlights
Omalizumab	Inflammation/ autoimmunity	MAB	Humanized IgG1, kappa	IgE	Soluble	Linear over 0.5 mg/kg	26 days (asthma) 24 days (CIU)	2.4 mL/day/kg (asthma); 3.0 mL/day/kg (CIU)	Apparent Vd = 78 ± 32 mL/ kg; *F* = 62%	SC injection; Asthma: mg dose based on weight (kg) and IgE level (IU/mL), CIU: flat mg dose
Reslizumab	Inflammation/ autoimmunity	MAB	Humanized IgG4 kappa	IL-5	Soluble	Linear	24 days	7 mL/h	5 L	IV infusion,mg/ kg dose
Rilonacept	Inflammation/ autoimmunity	Fusion protein	hIgG1	IL-1β	Soluble	NR	7.6 days	CL/F: 0.866 L/day	Vz/F: 9.73 L	SC injection, flat mg dose
Secukinumab	Inflammation/ autoimmunity	MAB	hIgG1 kappa	IL-17A	Soluble, cell-bound	Linear over 25–300 mg dose range	22–31 days	0.14–0.22 L/day	Vz: 7.10–8.60 L	SC injection, flat mg dose with loading dose
Siltuximab	Inflammation/ autoimmunity	MAB	Chimeric: mouse-human IgG1	IL-6	Soluble and cell-bound	Linear over a 2.8–11 mg/kg dose range	20.6 days range 14.2–29.7 days	0.23 L/day	70 kg male subject: 4.5 L	IV infusion, mg/ kg dose
Tocilizumab	Inflammation/ autoimmunity	MAB	Humanized IgG1	IL-6R	Soluble, cell-bound	Nonlinear	Up to 13 days	12.5 mL/h	6.4 L	IV infusion, mg/ kg dose
Ustekinumab[p]	Inflammation/ autoimmunity	MAB	hIgG1	IL-12, IL-23	Soluble	Linear	14.9–45.6 days	0.19 L/day	4.62 L	SC injection, flat mg dose
Vedolizumab	Inflammation/ Autoimmunity	MAB	Humanized IgG1	α4β7	Cell-bound	Linear and nonlinear	25 days at 300 mg	Linear CL: 0.157 L/day	5 L	IV infusion, flat mg dose
Alemtuzumab	Inflammation/ autoimmunity/ oncology	MAB	Humanized IgG1	CD52	Soluble	Nonlinear	MS: 14 days; CLL and NHL:11 h after single dose, 12 days following multiple doses[q]	NR	0.18 L/kg	IV infusion, flat mg dose
Rituximab	Inflammation/ autoimmunity/ oncology	MAB	Chimeric: mVar-hIgG1	CD20	Cell-bound	Linear	RA: 18 days (5.17–77.5 days); NHL: 22 days (6.1–52 days); CLL: 32 days (14–62 days)	RA: 0.335 L/day	RA: 3.1 L	IV infusion, mg/ m^2 dose
Asfotase alfa	Metabolic disorder	Fusion protein/ enzyme	Human TNSALP catalytic domain + hIgG1(Fc)	Hydrolyzes phosphor-monoesters	N/A	Linear	5 days	NR	NR	SC injection, mg/kg dose
Atezolizumab	Oncology	MAB	Non-glycosylated humanized IgG1	PD-L1	Soluble, cell-bound	Linear over 1 mg/kg to 20 mg/kg	27 days	0.2 L/kg	6.9 L	IV infusion, flat mg dose

Avelumab	Oncology	MAB	hIGg1 lambda	PD-L1	Soluble, cell-bound	Linear over 10–20 mg/kg	6.1 days at 10 mg/kg	0.59 L/day	4.72 L	IV infusion, mg/kg dose
Bevacizumab	Oncology	MAB	Humanized IgG1	VEGF	Soluble	Linear	20 days	0.207–0.262 L/day	2.66–3.25 L	IV infusion, mg/kg dose
Brentuximab vedotin	Oncology	ADC	Chimeric mVar-hIgG1	CD30	Cell-bound	Linear over 1.2–2.7 mg/kg	4.43 days	1.76 L/day[r]	8.21 L	IV infusion, mg/kg dose
Catumaxomab[l] (EU only)	Oncology	MAB	Chimeric: rat-mouse tri-functional MAB	EpCAM and CD3	Cell-bound	NR	2.5 days (range: 0.7–17 days)	NR	NR	IP infusion, flat μg dose
Cetuximab	Oncology	MAB	Chimeric: mVar-hIgG1	EGFR	Soluble	Nonlinear	4.8 days	0.02–0.08 L/h/m^2	2–3 L/m^2	IV infusion, mg/m^2 dose
Daratumumab	Oncology	MAB	hIgG1 kappa	CD38	Cell-bound	Nonlinear	18 ± 9 days (mono-therapy) 23 ± 12 days (combination therapy)	171.4 ± 95.3 mL/day	Vc: 4.7 ± 1.3 L (mono-therapy) 4.4 ± 1.5 L (combination therapy)	IV infusion, mg/kg dose
Denosumab	Oncology	MAB	hIgG2	RANKL	Cell-bound	Linear	28 days	CL_{linear} = 3.25 mL/h/66 kg	Vc = 2.62 L/66 kg; Vss = 3.96 L/66 kg[s]	SC injection, flat mg dose
Dinutuximab	Oncology	MAB	Chimeric: mVar-hIgG1 kappa	GD2 glycolipid	Cell-bound	NR	10 days	0.21 L/day	5.4 L	IV infusion, mg/m^2/day dose
Durvalumab	Oncology	MAB	hIgG1 kappa	PD-L1	Soluble, cell-bound	Linear over dose range of 3–20 mg/kg	17 days	CLss: 8.24 mL/h (clearance decreases over time)	5.6 L	IV infusion, mg/kg dose
Elotuzumab	Oncology	MAB	Humanized IgG1	CD319 (SLAMF7)	Cell-bound	Nonlinear	NR	0.5 mg/kg dose: 17.5 mL/day/kg; 20 mg/kg dose: 5.8 mL/day/kg	NR	IV infusion, mg/kg dose with loading dose
Gemtuzumab ozogamicin	Oncology	ADC	Humanized IgG4 kappa (hP67.6) + *N*-acetyl-gamma-calicheamicin (cytotoxin)	CD33	Cell-bound	Nonlinear	t1/2 hp67.6 MAB: after 1st dose = 62 h, after 2nd dose = 90 h	CLss hp67.6 MAB: after 1st dose = 0.35 L/h, after 2nd dose = 0.15 L/h	V1 = 6.31 L, V2 = 15.1 L for hp67.6 MAB	IV infusion, mg/m^2 dose
Ibritumomab tiuxetan	Oncology	MAB	Murine IgG1+ tiuxetan (chelator)	CD20	Cell-bound	NR	47 h[t]	NR	NR	IV injection over 10 min, mci/kg dose
Inotuzumab ozogamicin	Oncology	ADC	Humanized IgG4 kappa + *N*-acetyl-gamma-calicheamicin (cytotoxin)	CD22	Cell-bound	Nonlinear	12.3 days	CLss, 0.0333 L/h	12 L for ADC	IV infusion, mg/m^2 dose

Table 8.1 ■ (continued)

Name	Therapeutic area	Antibody/antibody derivatives		Target		PK				
		Type	Structure	Receptor/ antigen	Type	Behavior[b]	Elimination/ terminal half-life[c]	Clearance (CL)/ apparent CL	Volume of distribution (V and apparent V)[d]	Route/dosing highlights
Ipilimumab	Oncology	MAB	hIgG1	CTLA-4	Cell-bound	Linear	15.4 days	16.8 mL/h	7.21 L	IV infusion, mg/ kg dose
Necitumumab	Oncology	MAB	hIgG1 kappa	EGFR	Cell-bound	Nonlinear	14 days (after 800 mg on days 1 and 8 of each 21-day cycle)	14.1 mL/h after 800 mg on days 1 and 8 of each 21-day cycle	7.0 L after 800 mg on Days 1 and 8 of each 21-day cycle	IV infusion, flat mg dose
Nivolumab	Oncology	MAB	hIgG4 kappa	PD-1	Cell-bound	Linear	25 days	8.2 mL/h	6.8 L	IV infusion, flat mg dose
Obinutuzumab	Oncology	MAB	Humanized IgG1 with reduced fucose content	CD20	Cell-bound	Linear within recommended dose range	CLL patients: 25.5 days NHL patients: 35.3 days	CLL: 0.11 L/day; NHL: 0.08 L/ day (both values after TMDD saturation)	CLL: 4.1 L NHL: 4.3 L	IV infusion, flat mg dose
Ofatumumab	Oncology	MAB	hIgG1 kappa	CD-20	Cell-bound	Nonlinear	14 days	0.01 L/h	1.7–5.1 L	IV infusion, flat mg dose
Olaratumab	Oncology	MAB	hIgG1	PDGFR-α	Cell-bound	NR	11 days (range 6–24 days)	0.56 L/day	7.7 L	IV infusion, mg/ kg dose
Panitumumab[u]	Oncology	MAB	hIgG2	EGFR	Cell-bound	Nonlinear	7.5 days	4.9 mL/day/kg	82 mL/kg	IV infusion, mg/ kg dose
Pembrolizumab	Oncology	MAB	hIgG4 kappa	PD-1	Cell-bound	Linear over 2–10 mg/kg dose range	22 days	252 mL/day after first dose, 195 mL/day at steady state (geometric mean)	6.0 L	IV infusion, flat mg dose
Pertuzumab	Oncology	MAB	Humanized IgG1	HER2	Cell-bound, shed	Linear over 2-25 mg/kg dose range	18 days[v]	0.235 L/day[v]	5.57 L	IV infusion, flat mg dose
Ramucirumab	Oncology	MAB	hIgG1	VEGFR2	Cell-bound	Linear	14 days	0.015 L/h	NR	IV infusion, mg/ kg dose
Tositumomab	Oncology	MAB (radiolabeled)	mIgG2α	CD20	Cell-bound	Nonlinear	NR	68.2 mL/h	NR	IV infusion, flat mg dose
Trastuzumab	Oncology	MAB	Humanized IgG1	HER2	Cell-bound, shed	Nonlinear	NR	0.173–0.283 L/ day (breast cancer) 0.189–0.337 L/ day (gastric cancer)[w]	6 L (breast cancer) 6.6 L (gastric cancer)	IV infusion, mg/ kg dose
Trastuzumab emtansine	Oncology	ADC	Humanized IgG1 + emtansine (cytotoxin)	HER2	Cell-bound, shed	Linear at dose ≥2.4 mg/kg	4 days for ADC	0.68 L/day For ADC	3.13 L for ADC	IV infusion, mg/ kg dose

Ziv-aflibercept	Oncology	Fusion protein	Human VEGF receptors 1 and 2 ligand-binding ECD + hIgG1 (Fc)	hVEGF-A, hVEGF-B, hPIGF	Soluble	Linear	6 days (range 4–7 days)	NR	NR	IV infusion, mg/kg dose
Aflibercept	Ophthalmology	Fusion protein	hVEGF receptors 1 and 2 ECDs + human IgG1 (Fc)	VEGF-A, PlGF	Soluble	NR	5–6 days after IV	NR	6 L after IV	Intravitreal, flat mg dose
Ranibizumab	Ophthalmology	Fragment	humanized IgG1κ	VEGF	Soluble	NR	9 days	NR	NR	Intravitreal injection, flat mg dose
Basiliximab	Transplantation	MAB	Chimeric: mVar-hIgG1	CD25	Cell-bound	NR	4.1 days[x]	75 mL/h[x]	5.5–13.9 L	IV bolus or infusion, flat mg dose
Belatacept	Transplantation	Fusion protein	hCTLA-4 ECD + hFc (hinge)	CD80, CD86	Cell-bound	Linear	9.8 days	0.49 mL/h/kg	0.11 L/kg	IV infusion, mg/kg dose
Daclizumab	Transplantation	MAB	humanized IgG1	CD25	Cell-bound	Linear	20 days	15 mL/h	5.9 L	IV infusion, mg/kg dose
Muromonab-CD3	Transplantation	MAB	mIgG2α	CD3	Cell-bound	NR	0.75 days[y]	NR	NR	IV bolus, flat mg dose

ADC antibody-drug conjugate, *CD* cluster of differentiation, *CDR* complementarity determining region, *CLL* chronic lymphocytic leukemia, *CTLA* cytotoxic T lymphocyte-associated antigen, *ECD*, extracellular domain, *EGFR* epidermal growth factor receptor, *CLss* clearance at steady-state, *F* bioavailability, *Fab* antigen-binding fragment, *Fc* constant fragment, *HER2* human epidermal growth factor receptor 2, *Ig* immunoglobulin, *IL* interleukin, *IM* intramuscular, *IV* intravenous, *LFA* lymphocyte function-associated antigen, *MAB* monoclonal antibody, *MS* multiple sclerosis, *mVar* murine variable, *NA* information not available or not found, *NHL* Non-Hodgkin lymphoma, *NR* information not reported, *PD-1* programmed cell death 1 receptor, *PDGFR* prostaglandin, *PIGF* phosphatidylinositol-glycan biosynthesis class F protein, *RA* rheumatoid arthritis, *RANKL* receptor activator of nuclear factor kappa-B ligand, *RSV* respiratory syncytial virus, *SC* subcutaneous, *TNSALP* tissue non-specific alkaline phosphatase, *TNF* tumor necrosis factor, *V1* volume of distribution of central compartment, *V2* volume of distribution of peripheral compartment, *Vc* volume of central compartment, *VEGF* vascular endothelial growth factor, *Vss* volume of distribution at steady state, *Vz* volume of distribution during the terminal phase

[a]Source: prescribing information (not shown) and/or additional references as shown

[b]Where PK are nonlinear, parameters are reported at usual clinical dose

[c]Terminal t1/2 reported for linear PK only

[d]Volume or apparent volume of distribution at steady state, unless otherwise indicated

[e]Kleiman et al. (1995) and Mager et al. (2003)

[f]Kleiman et al. (1995) and Mager et al. (2003)

[g]CDER (2015)

[h]Hervey and Keam (2006)

[i]Weisman et al. (2003)

[j]In 2011, manufacturing, distribution and sales of Amevive were halted during a supply disruption. According to the manufacturer, Astellas Pharma US, Inc., the decision to cease Amevive sales was neither the result of any specific safety concern nor of any FDA-mandated or voluntary product recall

[k]Kovarik et al. (2001) and Kovalenko et al. (2016)

[l]Withdrawn from market

[m]Joshi et al. (2006)

[n]Lee et al. (2003)

[o]Cornillie et al. (2001)

[p]Zhu et al. (2009)

[q]Morris et al. (2003)

[r]Younes et al. (2010)

[s]Gibiansky et al. (2012)

[t]Wiseman et al. (2001)

[u]Ma et al. (2009)

[v]Garg et al. (2014)

[w]Kirschbrown et al. (2017)

[x]Kovarik et al. (2001)

[y]Hooks et al. (1991)

chapter provides a general introduction to Chaps. 23, 25, and 26, where the currently marketed MABs and MAB derivatives including antibody fragments, fusion proteins and ADCs are discussed in the context of their therapeutic applications. Efalizumab (anti-CD11a), a MAB marketed as an anti-psoriasis drug in the US and EU, was chosen to illustrate the application of PK/PD principles in the drug development process.

ANTIBODY STRUCTURE AND CLASSES

Antibodies, or immunoglobulins (Igs), are roughly Y-shaped molecules or combinations of such molecules. There are five major classes of Ig: IgG, IgA, IgD, IgE, and IgM. Table 8.2 summarizes the characteristics of these molecules, particularly their structure (monomer, dimer, hexamer, or pentamer), molecular weight (ranging from ~150 to ~1150 kDa), and functions (e.g., activate complement, FcγR binding). Among these classes, IgGs and their derivatives form the framework for the development of therapeutic antibodies. Figure 8.1 depicts the general structural components of IgG and a conformational structure of efalizumab. An IgG molecule has four peptide chains, including two identical heavy (H) chains (50–55 kDa) and two identical light (L) chains (25 kDa), which are linked via disulfide (S–S) bonds at the hinge region. The first ~110 amino acids of both chains form the variable regions (V_H and V_L) and are also the antigen-binding regions. Each V domain contains three short stretches of

Property		IgA		IgG				IgM	IgD	IgE
Serum concentration in adult (mg/mL)		IgA1	IgA2	IgG1	IgG2	IgG3	IgG4			
		1.4–4.2	0.2–0.5	5–12	2–6	0.5–1	0.2–1	0.25–3.1	0.03–0.4	0.0001–0.0002
Molecular form		Monomer, dimer		Monomer				Pentamer, hexamer	Monomer	Monomer
Functional valency		2 or 4		2				5 or 10	2	2
Molecular weight (kDa)		160 (m), 300 (d)	160 (m), 350 (d)	150	150	160	150	950 (p)	175	190
Serum half-life (days)		5–7	4–6	21–24	21–24	7–8	21–24	5–10	2–8	1–5
% total IgG in adult serum		11–14	1–4	45–53	11–15	3–6	1–4	10	0.2	50
Function	Activate classical complement pathway	–		+	±	++	–	+++	–	–
	Activate alternative complement pathway	+	–	–	–	–	–	–	–	–
	Cross placenta	–		+	±	+	+	–	–	–
	Present on membrane of mature B cell	–		–	–	–	–	+	–	+
	Bind to Fc receptors of phagocytes	–		++	±	++	+	+	–	–
	Mucosal transport	++		–	–	–	–	+	–	–
	Induces mast cell degranulation	–		–	–	–	–	–	+	–
Biological properties		Secretory Ig, binds to polymeric Ig receptor		Placental transfer, secondary antibody for most response to pathogen, binds macrophage and other phagocytic cells by Fcγ receptor				Primary antibody response, some binding to polymeric Ig receptor, some binding to phagocytes	Mature B cell marker	Allergy and parasite reactivity, binds FcεR on mast cells and basophiles

Table 8.2 ■ Important properties of endogenous immunoglobulin subclass (Goldsby et al. 1999; Kolar and Capra 2003)

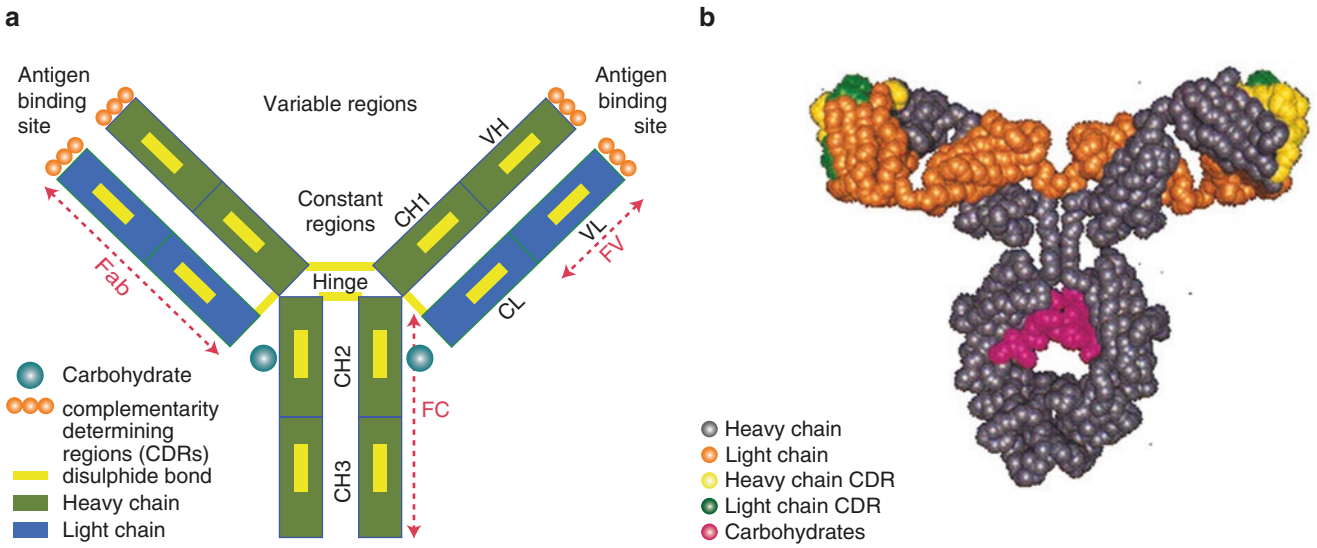

Figure 8.1 ■ (**a**) IgG1 antibody structure. Antigen is bound via the variable range of the antibody, whereas the Fc part of the IgG determines the mode of action (also called effector function). (**b**) Example of a conformational structure: efalizumab (anti-CD11a). *H chain* heavy chain consisting of VH, CH1, CH2, CH3; *L chain* light chain consisting of VL, CL; *VH, VL* variable light and heavy chain; *CHn, CL* constant light and heavy chain; *Fv* variable fraction; *Fc* crystallizable fraction; *Fab* antigen-binding fraction (http://people.cryst.bbk.ac.uk/~ubcg07s/gifs/IgG.gif)

peptide with hypervariable sequences (HV1, HV2, and HV3), known as complementarity determining regions (CDRs), i.e., the region that binds antigen. The remaining sequences of each light chain consist of a single constant domain (C_L). The remainder of each heavy chain contains three constant regions (C_{H1}, C_{H2}, and C_{H3}). Constant regions are responsible for effector recognition and binding. IgGs can be further divided into four subclasses (IgG1, IgG2, IgG3, and IgG4). The differences among these subclasses are also summarized in Table 8.2.

■ Murine, Chimeric, Humanized, and Fully Human MABs

The first therapeutic MABs were murine MABs produced via hybridomas; however, these murine MABs easily elicited formation of neutralizing human anti-mouse antibodies (HAMA) (Kuus-Reichel et al. 1994). With the advancement of technology, murine MABs have been engineered further to chimeric (mouse CDR, human Fc), humanized, and fully human MABs (Fig. 8.2). Murine MABs, chimeric MABs, humanized MABs, and fully human MABs have 0%, ~60–70%, ~90–95%, and ~100% sequence similarity to human MABs, respectively. Decreasing the xenogenic portion of the MAB potentially reduces the immunogenic risks of generating anti-drug antibodies (ADAs). Muromonab-CD3 (Orthoclone OKT3), a first-generation MAB of murine origin, has shown efficacy in the treatment of acute transplant rejection and was the first MAB licensed for use in humans. It is reported that 50% of the patients who received OKT3 produced

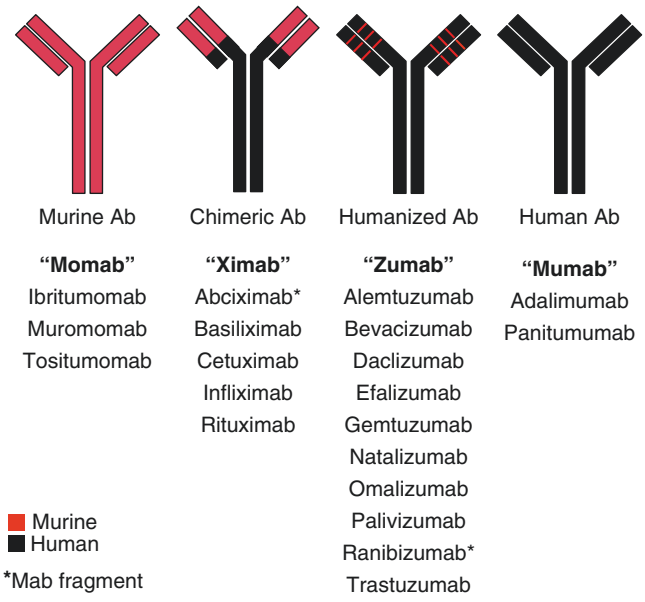

Figure 8.2 ■ Different generations of therapeutic antibodies

HAMA after the first dose. HAMA interfered with OKT3's binding to T cells, thus decreasing the therapeutic efficacy of the MAB (Norman et al. 1993). Later, molecular cloning and the expression of the variable region genes of IgGs facilitated the generation of engineered antibodies. A second generation of MABs, chimeric MABs, consists of human constant regions and mouse variable regions. The antigen specificity of a chimeric MAB is the same as the parental mouse antibody; however, the human Fc region renders a longer

in vivo half-life than the parent murine MAB, and similar effector functions as a human antibody. Currently, there are 9 chimeric MABs, fragments and ADCs on the market (abciximab, basiliximab, cetuximab, dinutuximab, infliximab, obiltoxaximab, rituximab, siltuximab, and brentuximab vedotin). These MABs can still induce human anti-chimeric antibodies (HACA). For example, about 61% of patients who received infliximab had a HACA response associated with shorter duration of therapeutic efficacy and increased risk of infusion reactions (Baert et al. 2003). The development of ADAs appears to be different across indications. For example, 6 of 17 patients with systemic lupus erythematosus receiving rituximab developed high-titer HACA (Looney et al. 2004), whereas only 1 of 166 B cell depleted lymphoma patients developed HACA (McLaughlin et al. 1998). Humanized MABs contain significant portions of human sequence except the CDR which is still of murine origin. There are more than 25 humanized MABs (including ADCs) on the market (see Table 8.1). The incidence of ADAs (in this case, human anti-human antibodies or HAHAs), was greatly decreased for these humanized MABs. Trastuzumab has a reported a HAHA incidence of ~0.1% (1 of 903 cases) (Herceptin (Trastuzumab) Prescribing Information 2006), but daclizumab had HAHA rate as high as 34% (Zenapax (Daclizumab) Prescribing Information 2005). Another way to achieve full biocompatibility of MABs is to develop fully human antibodies, which can be produced by two approaches: through phage-display library or by using transgenic animals, such as the XenoMouse® or Trianni Mouse™ (Weiner 2006; Trianni.com 2018). Adalimumab is the first licensed fully human MAB generated using a phage-display library. Adalimumab was approved in 2002 and 2007 for the treatment of rheumatoid arthritis (RA) and Crohn's diseases, respectively (Humira (Adalimumab) Prescribing Information 2007). However, despite its fully human antibody structure, the incidence of HAHA was about 5% (58 of 1062 patients) in three randomized clinical trials with adalimumab (Cohenuram and Saif 2007; Humira (Adalimumab) Prescribing Information 2007). Panitumumab is the first approved fully human MAB generated using transgenic mouse technology. HAHA responses have been reported as less than 1% by an acid dissociation bridging enzyme-linked immunosorbent assay (ELISA) in clinical trial after chronic dosing with panitumumab to date (Vectibix (Panitumumab) Prescribing Information 2015; Cohenuram and Saif 2007). Of note, typically ADAs are measured using ELISA, and the reported incidence rates of ADAs for a given MAB can be influenced by the sensitivity and specificity of the assay. Additionally, the observed incidence of ADA positivity in an assay may also be influenced by several other factors, including sample handling, timing of sample collection, concomitant medications, and underlying disease. For these reasons, comparison of the incidence of ADAs to a specific MAB with the incidence of ADAs to another product may be misleading.

■ Key Structural Components of MABs

Proteolytic digestion of antibodies releases different fragments termed Fv (fragment variable), Fab (fragment antigen binding), and Fc (fragment crystallization) [reviewed by Wang et al. (2007)]. These fragments can also be generated by recombinant engineering. Treatment with papain generates two identical Fab's and one Fc. Pepsin treatment generates a F(ab')2 and several smaller fragments. Reduction of F(ab')2 will produce two Fab fragments. The Fv consists of the heavy chain variable domain (V_H) and the light chain variable domain (V_L) held together by strong noncovalent interaction. Stabilization of the Fv by a peptide linker generates a single chain Fv (scFv).

■ Modifying Fc Structures

The Fc regions of MABs play a critical role not only in their function but also in their disposition in the body. MABs elicit effector functions, including antibody-dependent cellular cytotoxicity (ADCC), antibody-dependent cellular phagocytosis (ADCP) and complement-dependent cytotoxicity (CDC), following interaction between their Fc regions and different Fcγ receptors and complement fixation (C1q, C3b). The CH2 domain and the hinge region joining CH1 and CH2 have been identified as the crucial regions for binding to FcγR (Presta 2002; Presta et al. 2002). Engineered MABs with enhanced or decreased ADCC, ADCP and CDC activity have been produced by manipulation of the critical Fc regions. Umana et al. (1999) engineered an anti-neuroblastoma IgG1 with enhanced ADCC activity compared with wild type (WT). Shields et al. (2001) demonstrated that selected IgG1 variants with improved binding to FcγRIIIA showed enhanced ADCC by peripheral blood monocyte cells and natural killer cells. These findings indicate that Fc-engineered antibodies may have important applications for improving therapeutic efficacy. It was found that the FcγRIIIA gene dimorphism generates two allotypes, FcγRIIIa-158V and FcγRIIIa-158F, and the polymorphism in FcγRIIIA is associated with favorable clinical response following rituximab administration in non-Hodgkin's lymphoma patients (Cartron et al. 2004; Dall'Ozzo et al. 2004). Recently, obinutuzumab, an anti-CD20 MAB with enhanced effector functions as compared to rituximab, was approved for the treatment of patients with previously untreated chronic lymphocytic leukemia (CLL) and patients with

follicular lymphoma (FL) who relapsed after, or are refractory to, a rituximab-containing regimen. The efficacy of antibody-interleukin 2 fusion protein (Ab-IL2) was improved by reducing its interaction with Fc receptors (Gillies et al. 1999). In addition, the Fc portion of MABs also binds to FcRn (named based on its discovery in neonatal rats), an Fc receptor belonging to the major histocompatibility complex structure, which is involved in IgG transport and clearance (CL) (Junghans 1997). Engineered MABs with a decreased or increased FcRn binding affinity have been investigated for its potential to modify the pharmacokinetic behavior of MABs (see the section on Clearance for details).

Antibody Derivatives: F(ab')2, Fab, Antibody-Drug Conjugates and Fusion Proteins

The fragments of antibodies [Fab, F(ab')2, and scFv] have a shorter half-life compared with the corresponding full-sized antibodies. scFv can be further engineered into a dimer (diabody, ~60 kDa), or trimer (triabody, ~90 kDa). Two diabodies can be further linked together to generate a bispecific tandem diabody (tandab). A single Fab can be fused to a complete Fc engineered to form a single arm MAB, which is monovalent. Figure 8.3 illustrates the structure of different antibody fragments. Of note, abciximab, idarucizumab and ranibizumab are three Fabs approved by FDA. Abciximab is a chimeric Fab used for keeping blood from clotting that has a 20–30 min half-life in serum and 4-h half-life in platelets (Schror and Weber 2003). Ranibizumab, administrated via intravitreal injection, was approved for the treatment of macular degeneration in 2006 and exhibits a vitreous elimination half-life of 9 days (Albrecht and DeNardo 2006).

The half-life of Fc fragments is more similar to that of full-sized IgGs (Lobo et al. 2004). Therefore, Fc portions of IgGs have been used to form fusions with molecules such as cytokines, growth factor enzymes, or the ligand-binding region of receptor or adhesion molecules to improve their half-life and stability. There are ten Fc fusion proteins currently on the market [abatacept, aflibercept, alefacept, alprolix, antihemophilic factor (recombinant) Fc fusion protein, belatacept, dulaglutide, etanercept, rilonacept and ziv-aflibercept]. Etanercept, a dimeric fusion molecule consisting of the TNF-α receptor fused to the Fc region of human IgG1, has a half-life of approximately 70–100 h (Zhou 2005), which is much longer than that of the TNF-α receptor itself (30 min to ~2 h) (Watanabe et al. 1988).

Antibodies and antibody fragments can also be linked covalently with cytotoxic radionuclides or drugs to form radioimmunotherapeutic (RIT) agents or ADCs (Fig. 8.4), respectively. In each case, the antibody is used as a delivery mechanism to selectively target the cytotoxic moiety to tumors (Prabhu et al. 2011; Girish and Li 2015). For both ADCs and RIT agents, the therapeutic strategy involves selective delivery of a cytotoxin (drug or radionuclide) to tumors via the antibody. As targeted approaches, both technologies exploit the overexpression of target on the surface of the cancer cells and thereby minimize damage to normal tissues. Such approaches are anticipated to minimize the significant side effects encountered when cytotoxic small molecule drugs or radionuclides are administered as single agents, thus leading to enhanced therapeutic windows. However, important distinctions exist between these two therapeutic modalities. For example, ADCs usually require internalization into the endosomes and/or lysosomes for efficacy, while RIT agents are often able to emit beta or gamma radiation, even from the cell surface, to achieve cell killing following direct binding to membrane antigens. Furthermore, RIT can deliver high levels of radiation even with very low doses of radioimmunoconjugate. Importantly, most clinically successful ADC and RIT agents to date have been against hematologic tumors (Boswell and Brechbiel 2007). Trastuzumab emtansine is the only ADC approved in a solid tumor indication

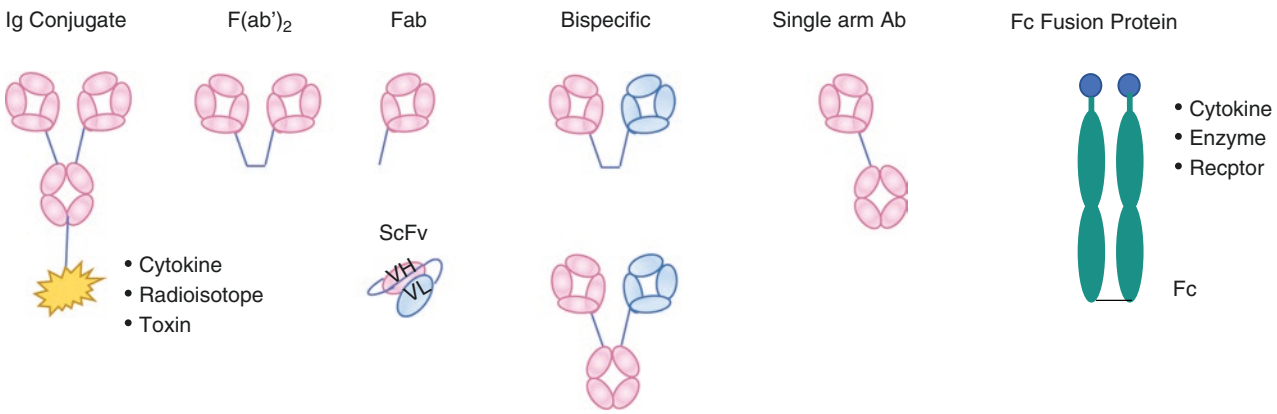

Figure 8.3 ■ Schematic representation of antibody derivatives: Ig conjugate, F(ab')2, Fab, scFv, bispecfic Ab, single arm Ab, and Fc fusion proteins

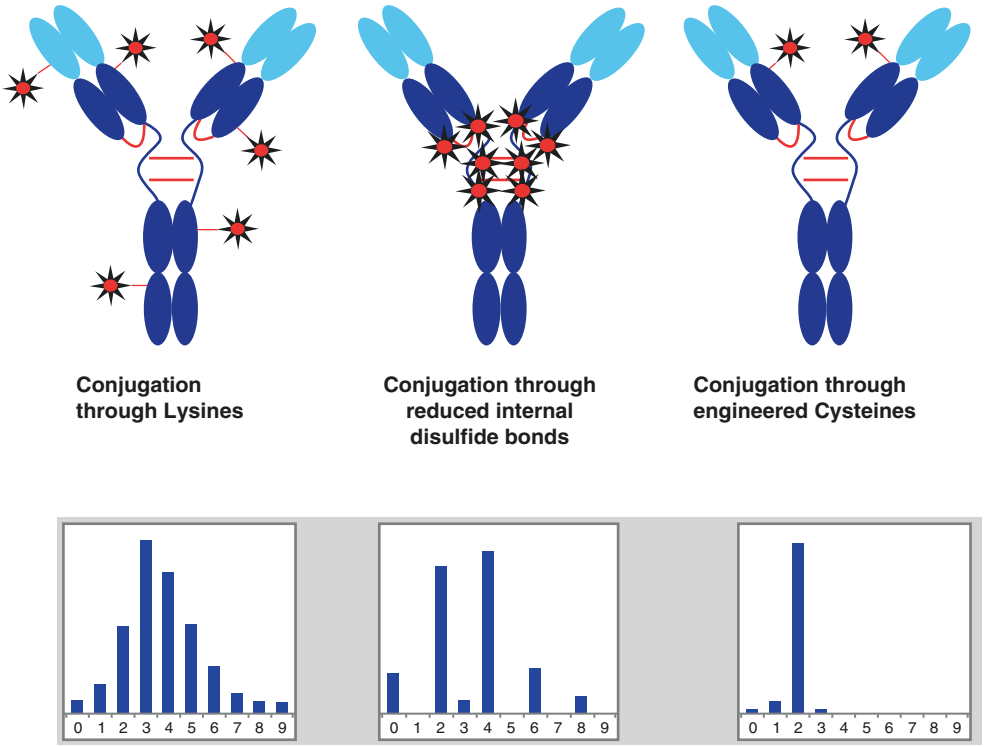

Figure 8.4 ■ Schematic of ADC structures. ADCs are a heterogeneous mixture of different drug-to-antibody ratio (DAR) species, with individual molecules exhibiting a range of DARs (Adapted with permission from Kaur et al., Mass Spectrometry of Antibody-Drug Conjugates in Plasma and Tissue in Drug Development. In *Characterization of Protein Therapeutics Using Mass Spectrometry*, 2013. Guodong Chen, Ed., Springer Press, New York, NY, pp 279–304)

(LoRusso et al. 2011). Various impediments to the delivery of antibodies and other macromolecules to solid tumors have been widely discussed and studied, especially in the context of microspatial distribution (Thurber et al. 2008).

Currently, there are four ADCs on the market. Gemtuzumab ozogamicin (Dowell et al. 2001), an anti-CD33 MAB linked to the cytotoxic antitumor antibiotic drug calicheamicin, became the first approved ADC in 2000 when it was granted accelerated approval for the treatment of acute myelogenous leukemia. Calicheamicin binds to the minor groove of DNA, causing double-strand DNA breaks and resulting in inhibition of DNA synthesis. However, gemtuzumab ozogamicin was removed from the US market in June 2010 after subsequent confirmatory trials failed to verify clinical benefit and demonstrated safety concerns, including deaths. In September 2017, the FDA re-approved gemtuzumab ozogamicin with a lower recommended dose and a different schedule in combination with chemotherapy or on its own. Gemtuzumab ozogamicin's history underscores the importance of examining alternative dosing, scheduling, and administration of therapies for patients with cancer, especially in those who may be most vulnerable to the side effects of treatment. In August 2011, the FDA approved a second ADC, brentuximab vedotin, a CD30-directed MAB linked to the cytotoxic microtubule-disrupting agent MMAE, for treatment of Hodgkin's lymphoma and systemic anaplastic large-cell lymphoma. In February 2013, the FDA approved ado-trastuzumab emtansine, a human epidermal growth factor receptor (HER2)-targeted ADC for treatment of HER2-positive breast cancer (LoRusso et al. 2011). In August 2017, inotuzumab ozogamicin, a CD22-directed MAB linked to calicheamicin, was approved by FDA for the treatment of adults with relapsed or refractory B-cell precursor acute lymphoblastic leukemia.

The only current radioimmunotherapeutic agents licensed by the FDA are ibritumomab tiuxetan and tositumomab plus ^{131}I-tositumomab, both for non-Hodgkin's lymphoma. Both of the above intact murine MABs bind CD20 and carry a potent beta particle-emitting radioisotope (^{90}Y for ibritumomab/tiuxetan and ^{131}I for tositumomab). In the case of ibritumomab, the bifunctional chelating agent, tiuxetan, is used to covalently link the radionuclide to the MAB ibritumomab. However, another approved anti-CD20 MAB, rituximab, is included in the dosing regimen as a non-radioactive pre-dose to improve the biodistribution of the radiolabeled MAB. Despite impressive clinical results, radioimmunotherapeutic MABs have not generated considerable commercial success; various financial, regulatory, and commercial barriers have been cited as contributing factors to this trend (Boswell and Brechbiel 2007).

MAB THERAPEUTIC MECHANISMS OF ACTION (MOAS)

The pharmacological effects of antibodies are first initiated by the specific interaction between antibody and antigen. MABs generally exhibit exquisite specificity for the target antigen. The binding site on the antigen, called the epitope, can be linear or conformational and may comprise continuous or discontinuous amino acid sequences. The epitope is the primary determinant of the antibody's modulatory functions, and depending on the epitope, the antibody may exert antagonist or agonist effects, or it may be nonmodulatory. The epitope may also influence the antibody's ability to induce ADCC and CDC. MABs exert their pharmacological effects via multiple mechanisms that include direct modulation of the target antigen, CDC and ADCC, ADCP, apoptosis, delivery of a radionuclide or immunotoxin to target cells and T cell activation using bispecific constructs.

■ Direct Modulation of Target Antigen

Examples of direct modulation of the target antigen include anti-TNFα, anti-IgE, and anti-CD11a therapies that are involved in blocking and removal of the target antigen. Most MABs act through multiple mechanisms and may exhibit cooperativity with concurrent therapies.

■ Complement-Dependent Cytotoxicity (CDC)

The complement system is an important part of the innate (i.e., nonadaptive) immune system. It consists of many enzymes that form a cascade with each enzyme acting as a catalyst for the next. CDC results from interaction of cell-bound MABs with proteins of the complement system. CDC is initiated by binding of the complement protein, C1q, to the Fc domain. The IgG1 and IgG3 isotypes have the highest CDC activity, while the IgG4 isotype lacks C1q binding and complement activation (Presta 2002). Upon binding to immune complexes, C1q undergoes a conformational change, and the resulting activated complex initiates an enzymatic cascade involving complement proteins C2 to C9 and several other factors. This cascade spreads rapidly and ends in the formation of the membrane attack complex (MAC), which inserts into the membrane of the target cell and causes osmotic disruption and lysis of the target. Figure 8.5 illustrates the mechanism for CDC with rituximab (a chimeric MAB that targets the CD20 antigen) as an example.

■ Antibody-Dependent Cellular Cytotoxicity (ADCC)

ADCC is a mechanism of cell-mediated immunity whereby an effector cell of the immune system actively lyses a target cell that has been bound by specific antibodies. It is one of the mechanisms through which antibodies, as part of the humoral immune response, can act to limit and contain infection. Classical ADCC is mediated by natural killer (NK) cells, monocytes, or macrophages, but an alternate ADCC is used by eosinophils to kill certain parasitic worms known as helminths. ADCC is part of the adaptive immune response due to its dependence on a prior antibody response. The typical ADCC involves activation of NK cells, monocytes, or macrophages and is dependent on the recognition of antibody-coated infected cells by Fc receptors on the surface of these cells. The Fc receptors recognize the Fc portion of antibodies such as IgG, which bind to the surface of a pathogen-infected target cell. The Fc receptor that exists on the surface of NK cell is called CD16 or FcγRIII. Once bound to the Fc receptor of IgG, the NK cell releases cytokines such as IFN-γ and cytotoxic granules like perforin and granzyme that enter the target cell and promote cell death

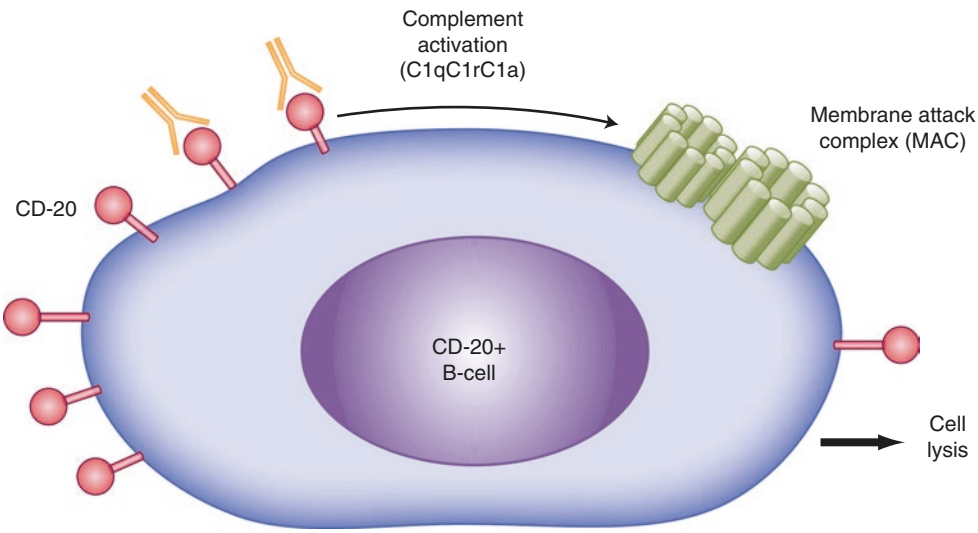

Figure 8.5 ■ An example of complement-dependent cytotoxicity (CDC), using a B cell lymphoma model, where the monoclonal antibody (MAB) rituximab binds to the receptor and initiates the complement system, also known as the "complement cascade." The end result is formation of a membrane attack complex (MAC), which leads to cell lysis and death

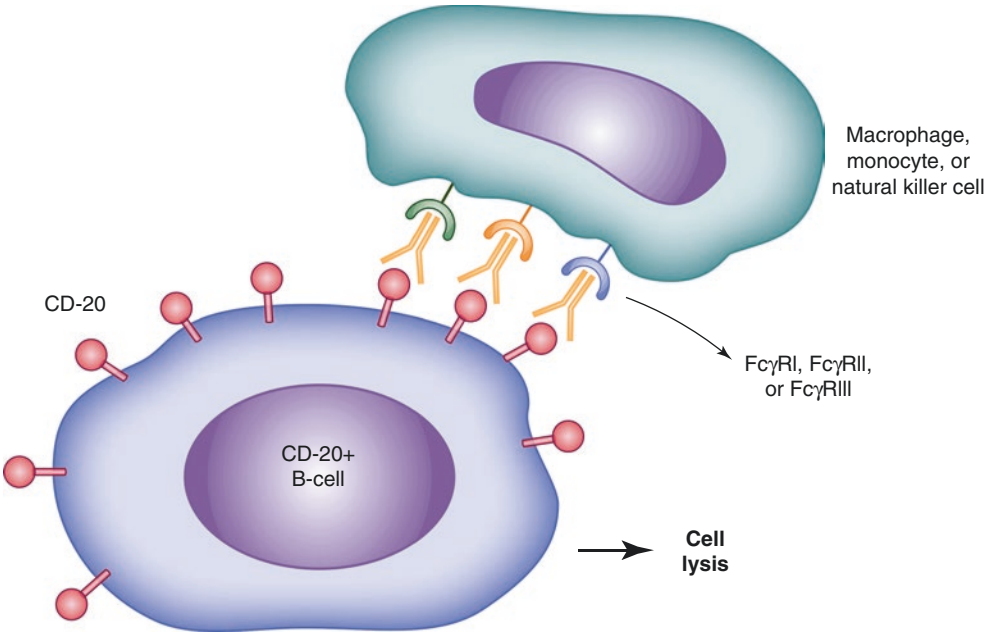

Figure 8.6 ■ An example of antibody-dependent cellular cytotoxicity (ADCC) and antibody-dependent cellular phagocytosis (ADCP). The monoclonal antibody (MAB) rituximab targets the CD20 antigen, which is expressed on a significant number of B cell malignancies. The Fc fragment of the MAB binds the Fc receptors found on effector cells such as monocytes, macrophages, and NK cells. These cells in turn either engulf the MAB-bound tumor cell (ADCP) or release cytotoxic agents such as perforin and granzymes, leading to destruction of the tumor cell (ADCC)

by triggering apoptosis. This is similar to, but independent of, responses by cytotoxic T cells. Figure 8.6 illustrates the mechanism for ADCC with rituximab as an example.

■ Antibody-Dependent Cellular Phagocytosis (ADCP)

ADCP is an immune effector function in which cells or particles opsonized with antibodies are engulfed by phagocytic effector cells, such as macrophages, following interactions between the Fc region of antibodies and Fcγ receptors on effector cells. In vivo, ADCP can be mediated by monocytes, macrophages, neutrophils and dendritic cells via all three types of activating Fcγ receptors: FcγRI, FcγRIIa, and FcγRIIIa. Studies have shown that MABs against tumor antigens induce phagocytosis of cancer cells in vitro, promote macrophage infiltration into tumors, and elicit macrophage-mediated destruction of tumors in mice (Weiskopf and Weissman 2015). ADCP is an important MOA of several antibody therapies for cancer, such as rituximab, obinutuzumab, and ocrelizumab. Engagement of Fcγ receptors expressed on phagocytic effector cells with antibodies bound to target cells triggers a signaling cascade leading to the engulfment of the antibody-opsonized tumor cells. Upon full engulfment, a phagosome is formed, which fuses with lysosomes, leading to acidification and digestion of the tumor cells. Figure 8.6 illustrates the mechanism for ADCP with rituximab as an example.

■ Apoptosis

MABs achieve their therapeutic effect through various mechanisms. In addition to the abovementioned effector functions, they can have direct effects in producing apoptosis or programmed cell death, which is characterized by nuclear DNA degradation, nuclear degeneration and condensation, and the phagocytosis of cell remains.

■ Targeted Delivery of Cytotoxic Drugs via ADCs

ADCs achieve their therapeutic effect through selectively delivering a potent cytotoxic agent to tumor cells (Girish and Li 2015). The MAB component enables the ADC to specifically bind to targeted cell surface antigens overexpressed on the tumor cells. After binding to the cell surface antigen, the ADC is internalized by the tumor cell, where it undergoes lysosomal degradation, leading to the release of the cytotoxic agent. Targeted delivery of cytotoxic drugs to tumors enables ADCs to potentially harness and improve their antitumor effect while minimizing their impact on normal tissues, thereby enhancing the benefit-risk profile.

■ $CD3^+$ T cell Activation Using Bispecific Constructs

CD3 bispecific constructs achieve their therapeutic effects through activating a patient's own $CD3^+$ T cells to attack target-positive tumor cells. CD3 bispecific constructs have one arm directed against the CD3 receptor on T cells and the other arm directed against a target cell surface antigen overexpressed by tumor cells (Mandikian et al. 2018). Simultaneous engagement of both arms results in formation of an immunologic synapse between a target tumor cell and a $CD3^+$ T cell, which leads to killing of the target tumor cells, either through direct killing by granzyme- and perforin-induced cell lysis or through cytokine release caused by T-cell activation.

TRANSLATIONAL MEDICINE/DEVELOPMENT PROCESS

The tight connection of basic to clinical sciences is an essential part of translational medicine, which aims to *translate* the knowledge of basic science into practical therapeutic applications for patients. This knowledge transfer is often referred to as the process of moving *from-bench-to-bedside*, emphasizing the transition of scientific advancements into clinical applications. This framework of translational medicine is applied during the discovery and drug development process of a specific MAB against a certain disease. It includes major steps such as identifying an important and viable pathophysiological target antigen to modify the disease in a beneficial way, producing MABs with structural elements providing optimal PK, preclinical safety and efficacy testing in relevant models, and finally clinical trials in patients. An overview of the development phases of the molecules comprising the preclinical activities is outlined in Fig. 8.7. Furthermore, the critical components of the entire MAB development process are explained in detail from a PK/PD perspective below.

■ Preclinical Safety Assessment of MABs

Preclinical safety assessment of MABs encounters unique challenges, as many of the classical evaluations employed for small molecules are not appropriate for protein therapeutics in general and MABs in particular. For example, in vitro genotoxicology tests such as the Ames and chromosome aberration assays are generally not conducted for MABs given their limited interaction with nuclear material and the lack of appropriate receptor/target expression in these systems. As MAB binding tends to be highly species specific, suitable animal models are often limited to nonhuman primates, and for this reason, many common in vivo models, such as rodent carcinogenesis bioassays and some safety pharmacology bioassays, are not viable for MAB therapeutic candidates. For general toxicology studies, cynomolgus and rhesus monkeys are most commonly employed and offer many advantages given their close phylogenetic relationship with humans; however, due to logistics, animal availability, and costs, group sizes tend to be much smaller than typically used for lower species, thus limiting statistical power. In some cases, alternative models are employed to enable studies in rodents. Rather than directly testing the therapeutic candidate, analogous MABs that can bind to target epitopes in lower species (e.g. mice) can be engineered and used as a surrogate MAB for safety evaluation (Clarke et al. 2004). Often the antibody framework amino acid sequence is modified to reduce antigenicity thus enabling longer-term studies (Albrecht and DeNardo 2006; Weiner 2006; Cohenuram and Saif 2007). Another approach is to use transgenic models that express the human receptor/target of interest (Bugelski et al. 2000), although results must be interpreted with caution as transgenic models often have altered physiology and typically lack historical background data for the model (Boswell et al. 2013). To address development issues that are specific to MABs and other

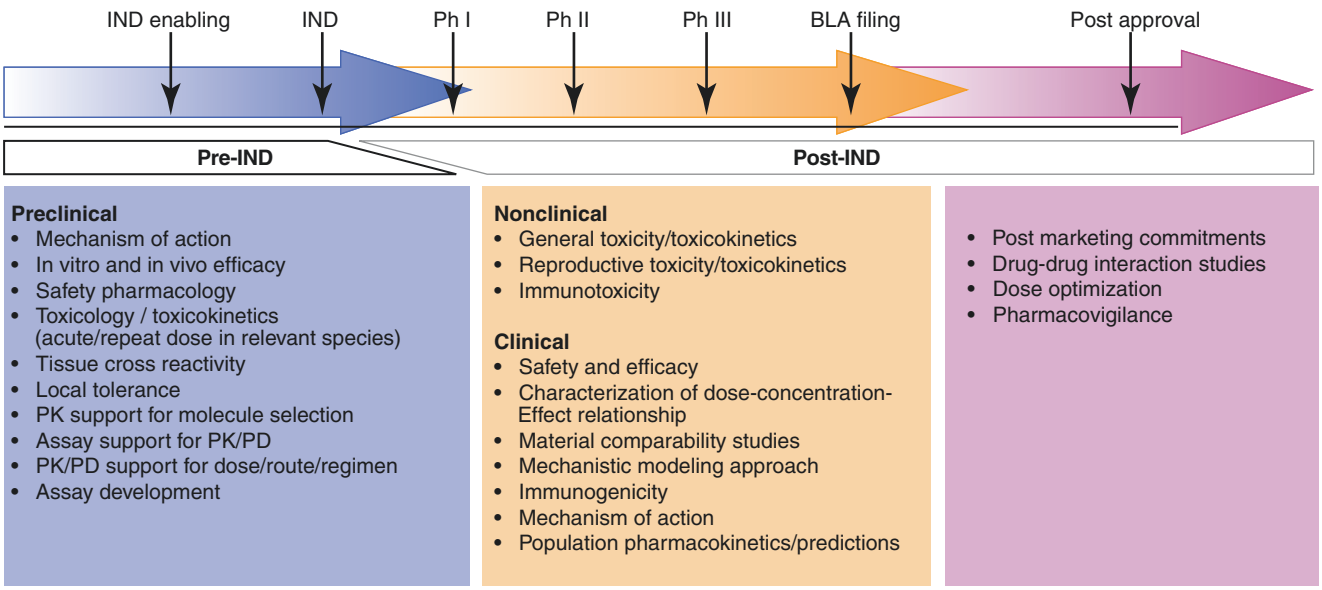

Figure 8.7 ■ Flowchart depicting high level PK/PD/toxicology study requirements during preclinical and clinical drug product development

protein therapeutics, the International Conference of Harmonization (ICH) has developed guidelines specific to the preclinical evaluation of biotechnology-derived pharmaceuticals (ICH 1997a, b).

For general safety studies, species selection is an important consideration given the exquisite species specificity often encountered with MABs. Model selection needs to be justified based on appropriate expression of the target epitope, appropriate binding affinity with the therapeutic candidate, and appropriate biologic activity in the test system. To aid in the interpretation of results, tissue cross-reactivity studies offer the ability to compare drug localization in both animal and human tissues. For MAB therapeutic candidates, a range of three or more dose levels are typically selected to attain pharmacologically relevant serum concentrations, to approximate levels anticipated in the clinic, and to provide information at doses higher than anticipated in the clinic. For most indications, it is important to include dose levels that allow identification of a no observable adverse effect level (NOAEL). If feasible, the highest dose should fall within the range where toxicity is anticipated; although, in practice, many MABs do not exhibit toxicity, and other factors limit the maximum dose. To best reflect human exposures, doses are often normalized and selected to match and exceed anticipated human therapeutic exposure in plasma, serum, or blood based upon the exposure parameters, area under the concentration-time curve (AUC), maximum concentration (C_{max}), or concentration immediately prior to next treatment (C_{trough}). The route of administration, dosing regimen, and dosing duration should be selected to best model the anticipated use in clinical trials (ICH 1997a, b).

To adequately interpret nonclinical study results, it is important to characterize ADA responses. For human MABs, ADA responses are particularly prominent in lower species but also evident in nonhuman primates albeit to a lesser degree, making these species more viable for chronic toxicity studies. ADAs can impact drug activity in a variety of ways. Neutralizing ADAs are those that bind to the therapeutic in a manner that prevents activity, often by inhibiting direct binding to the target epitope. Non-neutralizing antibodies may also indirectly impact drug activity, for example, rapid clearance of drug–ADA complexes can effectively reduce serum drug concentrations. In situations where prominent ADA responses are expected, administration of high-dose multiples of the anticipated clinical dose may overcome these issues by maintaining sufficient circulating concentrations of active drug when supported with sufficient safety margin. To properly interpret study results, it is important to characterize ADA incidence and magnitude, as the occurrence of ADA responses could mask toxicities. Alternatively, robust ADA responses may induce significant signs of toxicity, such as infusion-related anaphylaxis, that may not be predictive of human outcome where ADA formation is likely to be less of an issue. If ADA formation is clearly impacting circulating drug levels, ADA-positive individual animals are often removed from consideration when evaluating pharmacokinetic parameters to better reflect the anticipated PK in human populations.

■ Pharmacokinetics

A thorough and rigorous PK program in the early learning phase of preclinical drug development can provide a linkage between drug discovery and preclinical development. PK information can be linked to PD by mathematical modeling, which allows characterizing the time course of the effect intensity resulting from a certain dosing regimen. Antibodies often exhibit PK properties that are complex and different than those typically associated with small molecule drugs (Meibohm and Derendorf 2002). The PK of ADCs is more complex due to the presence of both an antibody component as well as a small molecule component. In the following sections, the basic characteristics of MAB and ADC PK are summarized in contrast to small molecule drugs.

The PK of antibodies and ADCs are very different from that of small molecules, as summarized in Table 8.3. Precise, sensitive, and accurate bioanalytical methods are essential for PK interpretation. However, for MABs, the immunoassays and bioassay methodologies are often less specific than assays used for small molecule drugs (e.g., LC/MS/MS). MABs are handled by the body very differently than are small molecules. In contrast to small molecule drugs, the typical metabolic enzymes and transporter proteins, such as cytochrome P450 and multidrug resistance (MDR) efflux pumps, are not involved in the disposition of MABs. Consequently, drug–drug interactions (DDI) at the level of these drug-metabolizing enzymes and transporters are not complicating factors in the drug development process of MABs and in general do not need to be addressed by in vitro and in vivo studies. Because of their large molecular weight, intact MABs are not usually cleared by the kidneys; however, renal clearance processes may play an important role in the elimination of molecules of smaller molecular weight such as Fab's and chemically derived small molecule drugs. The different *ADME* (*A*bsorption, *D*istribution, *M*etabolism, and *E*limination) processes comprising the PK of MABs are discussed separately to address their individual specifics.

Small Molecule Drugs	Monoclonal Antibodies	Antibody-Drug Conjugates
High potency and low specificity	Low potency and high specificity	High potency and high specificity
PK usually independent of PD	PK usually dependent of PD	Same as MAB
Binding generally nonspecific (can affect multiple enzymes)	Binding very specific for target protein or antigen	Same as MAB
Linear PK at low doses (usually therapeutic doses); nonlinear PK at high doses (after saturation of metabolic enzymes)	Nonlinear PK at low doses; linear PK at high doses after saturation of target	Same as MAB
Relatively short $t_{1/2}$ (hours)	Long $t_{1/2}$ (days or weeks)	Long $t_{1/2}$ of antibody; sustained delivery of small molecule (formation rate limited)
Oral delivery often possible	Need parenteral dosing. Subcutaeneous (SC) or intramusclular (IM) is possible	Need parenteral dosing. SC or IM has not been tested
Metabolism by cytochrome P450 or other phase I/ phase II enzymes	Catabolism by proteolytic degradation	Catabolism by proteolytic degradation; small molecule component can undergo excretion unchanged or metabolism by cytochrome P450 enzymes or other phase I/ phase II enzymes
Renal clearance often important	No renal clearance of intact antibody. May be eliminated by damaged kidneys. Antibody fragment might be eliminated by renal clearance.	Combination of mAb and small molecule; Released small molecule can be cleared renally and/or hepatically
High volume of distribution due to binding to tissues	Distribution usually limited to blood and extra-cellular space	Same as MAB
No immunogenicity	Immunogenicity may be seen	Same as MAB
Narrow therapeutic window	Large therapeutic window	Depends on potency of payload

Table 8.3 ■ Comparison of the pharmacokinetics between small molecule drugs, monoclonal antibodies and antibody-drug conjugates (Mould et al. 1999; Lobo et al. 2004; Roskos et al. 2004; Mould and Sweeney 2007; Kamath 2016)

Absorption

Most MABs are not administrated orally because of their limited gastrointestinal stability, lipophilicity, and size, all of which result in insufficient resistance against the hostile proteolytic gastrointestinal milieu and very limited permeation through the lipophilic intestinal wall. Therefore, intravenous (IV) administration is still the most frequently used route, which allows for immediate systemic delivery of a large volume of drug product and provides complete systemic availability. Subcutaneous (SC) administration, however, may offer a number of benefits over IV administration. Being less invasive and with a much shorter injection duration (2–7 min versus 30–90 min for IV infusion), and commonly with a fixed dose, SC dosing is expected to offer more convenience to patients compared to IV infusion. Additionally, IV infusion is typically administered in a hospital or physician's office; SC administration may allow self or healthcare professional-assisted home administration. Of note, 22 of the 75 FDA-approved MAB or MAB-derived therapies listed in Table 8.1 are administered by an extravascular route, either SC or IM. Aflibercept and ranibizumab are administered via intravitreal injection.

The absorption mechanisms of SC or IM administration are poorly understood. However, it is believed that the absorption of MABs after IM or SC injection is likely via lymphatic drainage due to its large molecular weight, leading to a slow absorption rate (see Chaps. 5 and 6). The bioavailability of MABs after SC or IM administration has been reported to be around 50–100% with maximal plasma concentrations observed 1–8 days following administration (Lobo et al. 2004). For example, following an IM injection, the bioavailability of alefacept was ~60% in healthy male volunteers; its C_{max} was threefold lower (0.96 versus 3.1 μg/mL), and its T_{max} was 30 times longer (86 versus 2.8 h) than a 30-min IV infusion (Vaishnaw and TenHoor 2002). Interestingly, differences in PK have also been observed between different sites of IM dosing. PAmAb, a fully humanized MAB against *Bacillus anthracis* protective antigen, has significantly different pharmacokinetics between IM-GM (gluteus maximus site) and IM-VL (vastus lateralis site) injection in healthy volunteers (Subramanian et al. 2005). The bioavailability of PAmAb is 50–54% for IM-GM injection and 71–85% for IM-VL injection (Subramanian et al. 2005). Of note, MABs appear to have greater bioavailability after SC administration in monkeys than in humans (Oitate et al. 2011). The mean bioavailability of adalimumab is 52–82% after a single 40 mg SC administration in healthy adult subjects, whereas it was observed to be 94–100% in monkeys. Similarly, the mean bioavailability of omalizumab is 66–71% after a single SC dose in patients with asthma versus 88–100% in monkeys (Oitate et al. 2011).

Although SC administration of MABs initially used low-volume injections (1–2 mL), in recent years, larger-volume injections (>2 mL) have been used, with and without permeation enhancers. SC injections of a viscous (5 cP) placebo buffer, characteristic of a high-concentration MAB formulation, at volumes of up to 3.5 mL had acceptable tolerability in healthy adult subjects at injection rates up to 3.5 mL/min (Dias et al. 2015a, b). Due to relatively large therapeutic doses (several hundred milligram), dosing volumes of high-concentration MABs may still be too large to facilitate a painless SC injection. Without co-injection of a permeation enhancer, large volume injections may produce swelling at the injection site, particularly in the thigh and arm. A permeation enhancer, such as recombinant human hyaluronidase (rHuPH20), reduces this swelling. Hyaluronidase is a 61-kD naturally-occurring enzyme that temporarily degrades hyaluronan in the skin and increases dispersion of the MAB over a greater area. Co-formulation of rHuPH20 with therapeutic proteins allows SC administration of larger injection volumes and potentially enhances absorption of the therapeutic protein into the systemic circulation (Frost 2007). Trastuzumab and rituximab have both been co-formulated with rHuPH20 to facilitate large-volume SC injections (Bittner et al. 2012). Trastuzumab is available as a 5-mL SC injection to be administered over 2–5 min, while rituximab is available at 11.7 or 13.4 mL injection volumes to be administered over 5 or 7 min, respectively.

Distribution

After reaching the bloodstream, MABs undergo biphasic elimination from serum, beginning with a rapid distribution phase. The volume of distribution of the rapid-distribution compartment is relatively small, approximating plasma volume. It is reported that the volume of the central compartment (Vc) is about 2–3 L, and the steady-state volume of distribution (Vss) is around 3.5–7 L for MABs in humans (Lobo et al. 2004; Roskos et al. 2004). The small Vc and Vss for MABs indicate that the distribution of MABs is restricted to the blood and extracellular spaces, which is in agreement with their hydrophilic nature and their large molecular weight, limiting access to the intracellular compartment surrounded by a lipid bilayer. Small volumes of distributions are consistent with relatively small tissue: blood ratios for most antibodies typically ranging from 0.1 to 0.5 (Baxter et al. 1995; Baxter et al. 1994; Berger et al. 2005). For example, the tissue-to-blood concentration ratios for a murine IgG1 MAB against the human ovarian cancer antigen CA125 in mice at 24 h after injection are 0.44, 0.39, 0.48, 0.34, 0.10, and 0.13 for the spleen, liver, lung, kidney, stomach, and muscle, respectively. Brain and cerebrospinal fluid are anatomically protected by blood–brain barriers. Although the blood-brain barrier was believed to be impaired in certain neurodegenerative disease states, recent work has brought this into question (Bien-Ly et al. 2015). Therefore, both compartments are very limited distribution compartments for MABs. For example, endogenous IgG levels in CSF were shown to be in the range of only 0.1–1% of their respective serum levels (Wurster and Haas 1994; Yadav et al. 2017; Yu et al. 2014).

It has been repeatedly noted that the reported Vss obtained by traditional non-compartmental or compartmental analysis may not be correct for MABs that primarily undergo catabolism within tissue (Lobo et al. 2004; Straughn et al. 2006; Tang et al. 2004). The rate and extent of MAB distribution will be dependent on the kinetics of MAB extravasation within tissue, distribution within tissue, and elimination from tissue. Convection, diffusion, transcytosis, binding, and catabolism are important determining factors for antibody distribution (Lobo et al. 2004). Therefore, Vss might be substantially greater than the plasma volume in particular for those MABs demonstrating high binding

affinity in the tissue. Different research groups have reported effects of the presence of specific receptors (i.e., antigen sink) on the distribution of MABs (Danilov et al. 2001; Kairemo et al. 2001; Bumbaca et al. 2012). Danilov et al. (2001) found in rats that an anti-PECAM-1 (anti-CD31) MAB showed tissue-to-blood concentration ratios of 13.1, 10.9, and 5.96 for the lung, liver, and spleen, respectively, 2 h after injection. Therefore, the true Vss of the anti-PECAM-1 is likely to be 15-fold greater than plasma volume.

Another complexity to consider is that tissue distribution via interaction with target proteins (e.g., cell surface proteins) and subsequent internalization of the antigen-MAB complex may be dose dependent. For the murine analog MAB of efalizumab, M17, a pronounced dose-dependent distribution was demonstrated by comparing tissue-to-blood concentration ratios for liver, spleen, bone marrow, and lymph node after a tracer dose of radiolabeled M17 and a high-dose treatment (Coffey et al. 2005). The tracer dose of M17 resulted in substantially higher tissue-to-blood concentration ratios of 6.4, 2.8, 1.6, and 1.3 for the lung, spleen, bone marrow, and lymph node, respectively, in mice at 72 h after injection. In contrast, the saturation of the target antigen at the high-dose level reduced the tissue distribution to the target independent distribution and resulted consequently in substantially lower tissue-to-blood concentration ratios (less than 1).

FcRn may play an important role in the transport of IgGs from plasma to the interstitial fluid of tissue. Recently, the data from Yip et al. increased understanding of FcRn's role in antibody PK and catabolism at the tissue level (Yip et al. 2014). They reported that distribution of the wild-type IgG and the variant with enhanced binding for FcRn were largely similar to each other in mice, but vastly different for the low-FcRn-binding variant due to its very low systemic exposure and widespread catabolism, particularly in liver and spleen. Ferl et al. (2005) reported that a physiologically based pharmacokinetic (PBPK) model, including the kinetic interaction between the MAB and the FcRn receptor within intracellular compartments, could describe the biodistribution of an anti-CEA MAB in a variety of tissue compartments such as plasma, lung, spleen, tumor, skin, muscle, kidney, heart, bone, and liver. FcRn was also reported to mediate the crossing of placental barriers by IgG (Junghans 1997) and the vectorial transport of IgG into the lumen of intestine (Dickinson et al. 1999) and lung (Spiekermann et al. 2002).

Clearance

Antibodies are mainly cleared by catabolism and broken down into peptide fragments and amino acids, which can be recycled—to be used as energy supply or for new protein synthesis. Due to the small molecular weight of antibodies fragments (e.g., Fab and Fv), elimination of these fragments is faster than for intact IgGs, and they can be filtered through the glomerulus and reabsorbed and/or metabolized by proximal tubular cells of the nephron (Lobo et al. 2004). Murine monoclonal anti-digoxin Fab, F(ab')2, and IgG1 have half-lives of 0.41, 0.70, and 8.10 h in rats, respectively (Bazin-Redureau et al. 1997). Several studies reported that the kidney is the major route for the catabolism of Fab and elimination of unchanged Fab (Druet et al. 1978; McClurkan et al. 1993).

Typically, IgGs have serum half-lives of approximately 21 days, resulting from CL values of about 3–5 mL/day/kg, and Vss's of 50–100 mL/kg. The exception is IgG3, which has a half-life of only 7 days. The half-life of IgG is much longer than that of other Igs (IgA, 6 days; IgE, 2.5 days; IgM, 5 days; IgD, 3 days). The FcRn receptor has been demonstrated to be a primary determinant of the disposition of IgG antibodies (Ghetie et al. 1996; Junghans 1997; Junghans and Anderson 1996). FcRn, which protects IgG from catabolism and contributes to the long plasma half-life of IgG, was first postulated by Brambell in 1964 (Brambell et al. 1964) and cloned in the late 1980s (Simister and Mostov 1989a, b). FcRn is a heterodimer comprising of a β_2m light chain and a MHC class I-like heavy chain. The receptor is ubiquitously expressed in cells and tissues. Several studies have shown that IgG CL in β_2m knockout mice (Ghetie et al. 1996; Junghans and Anderson 1996) and FcRn heavy chain knockout mice (Roopenian et al. 2003) is increased 10 to 15-fold, with no changes in the elimination of other Igs. Figure 8.8 illustrates how the FcRn receptor protects IgG from catabolism and contributes to its long half-life. The FcRn receptor binds to IgG in a pH-dependent manner: binding to IgG at the acidic pH (6.0) of the endosome and releasing IgG at physiological pH (7.4). The unbound IgG proceeds to the lysosome and undergoes proteolysis.

It has been demonstrated that IgG half-life is dependent on its affinity to FcRn receptors. The shorter half-life of IgG3 was attributed to its low binding affinity to the FcRn receptor (Junghans 1997; Medesan et al. 1997). Murine MABs have serum half-lives of 1–2 days in human. The shorter half-life of murine antibodies in human is due to their low binding affinity to the human FcRn receptor. It is reported that human FcRn binds to human, rabbit, and guinea pig IgG, but not to rat, mouse, sheep, and bovine IgG; however, mouse FcRn binds to IgG from all of these species (Ober et al. 2001). Interestingly, human IgG1 has greater affinity to murine FcRn (Petkova et al. 2006), which indicates potential limitations of using mice as preclinical models for human IgG1 pharmacokinetic evaluations.

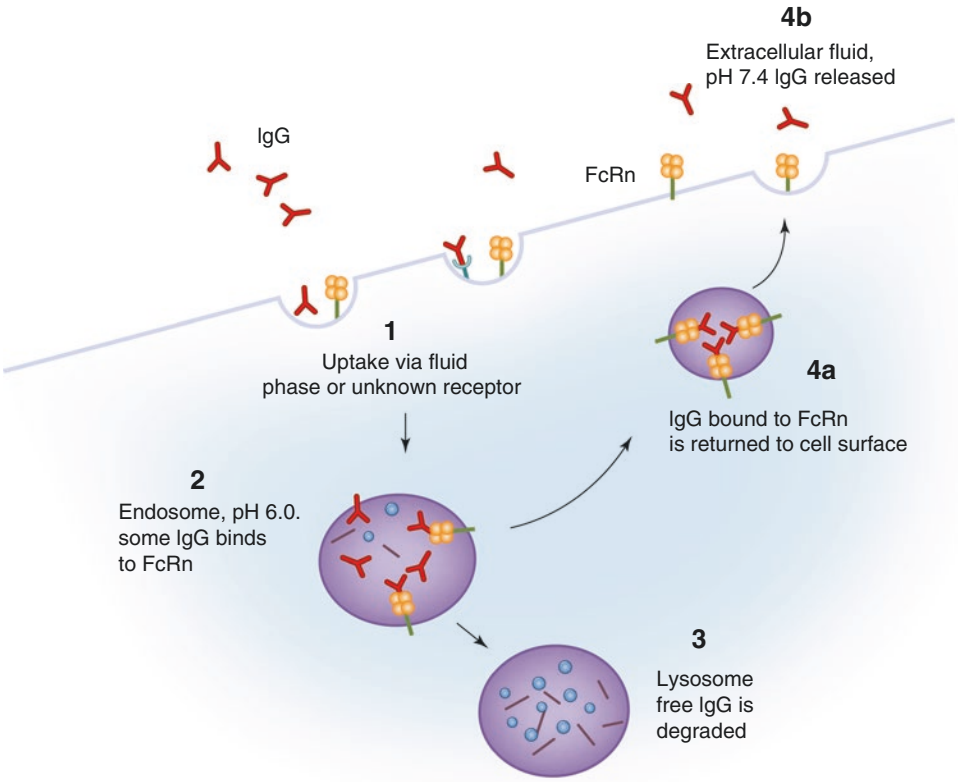

Figure 8.8 ■ Schematic disposition pathway of IgG antibodies via interaction with FcRn in endosomes. (1) IgGs enter cells by receptor-mediated endocytosis by binding of the Fc part to FcRn. (2) The intracellular vesicles (endosomes) fuse with lysosomes containing proteases. (3) Proteases degrade unbound IgG molecules, whereas IgGs bound to FcRn are protected. (4a) The intact IgG bound to FcRn is transported back to the cell surface and (4b) released back to the extracellular fluid

Ward's group confirmed that an engineered human IgG1 had disparate properties in murine and human systems (Vaccaro et al. 2006). Engineered IgGs with higher affinity to FcRn receptor have a two to three-fold longer half-life compared with WT in mice and monkeys (Hinton et al. 2006; Petkova et al. 2006). Two engineered human IgG1 mutants with enhanced binding affinity to human FcRn show a considerably extended half-life compared with WT in hFcRn transgenic mice (4.35 ± 0.53, 3.85 ± 0.55 days versus 1.72 ± 0.08 days) (Hinton et al. 2006; Petkova et al. 2006) found that the half-life of IgG1 FcRn mutants with increasing binding affinity to human FcRn at pH 6.0 is about 2.5-fold longer than the WT antibody in monkey (838 ± 187 h versus 336 ± 34 h).

Dose-proportional, linear CL has been observed for MAB against soluble antigens with low endogenous levels (such as TNF-α, IFN-α, VEGF, and IL-5). For example, linear PK has been observed for a humanized MAB directed to human interleukin-5 following IV administration over a 6000-fold dose range (0.05–300 mg/kg) in monkeys (Zia-Amirhosseini et al. 1999). The CL of rhuMAB against VEGF after IV dosing (2–50 mg/kg) ranged from 4.81 to 5.59 mL/day/kg and did not depend on dose (Lin et al. 1999). The mean total serum CL and the estimated mean terminal half-life of adalimumab were reported to range from 0.012 to 0.017 L/h and 10.0 to 13.6 days, respectively, for a 5-cohort clinical trial (0.5–10 mg/kg), with an overall mean half-life of 12 days (den Broeder et al. 2002). However, MABs against soluble antigens with high endogenous levels (such as IgE) exhibit nonlinear PK. The PK of omalizumab, an MAB against IgE, is linear only at doses greater than 0.5 mg/kg (Petkova et al. 2006; Xolair (Omalizumab) Prescribing Information 2006).

Elimination of MABs may also be impacted by interaction with the targeted cell-bound antigen, and this phenomenon was demonstrated by dose-dependent clearance and half-life. At low dose, MABs show a shorter half-life and a faster clearance due to receptor-mediated elimination. With increasing doses, receptors become saturated, the half-life gradually increases to a constant, and the CL gradually decreases to a constant. The binding affinity (K_d), antigen density, and antigen turnover rate may influence the receptor-mediated elimination. Koon et al. found a strong inverse correlation between CD25 cell expression and the apparent half-life of daclizumab (a MAB specifically binding to CD25) (Koon et al. 2006). It has been shown that the PK of murine antihuman CD3 antibodies may be determined by the disappearance of target antigen (Meijer et al. 2002). In monkeys and mice, clearance of SGN-40, a humanized anti-CD40 MAB, was much faster at low dose, suggesting nonlinear PK (Kelley et al. 2006). In addition, Ng et al. demonstrated that an anti-CD4 MAB (TRX-1) had ~fivefold faster CL at 1 mg/kg dose compared with 10 mg/kg

dose (37.4 ± 2.4 versus 7.8 ± 0.6 mL/day/kg) in healthy volunteers (Ng et al. 2006). They also found that receptor-mediated CL via endocytosis became saturated at higher doses; nonspecific clearance of TRX-1 contributed 8.6, 27.1, and 41.7% of total CL when dose was 1, 5, and 10 mg/kg, respectively.

In addition to FcRn and antigen–antibody interaction, other factors may also contribute to MAB elimination (Roskos et al. 2004; Tabrizi et al. 2006; Lobo et al. 2004):

1. *Immunogenicity*: The elimination of MABs in humans may increase with increasing level of immunogenicity (Tabrizi et al. 2006; Ternant and Paintaud 2005).
2. *Degree and the nature of glycosylation*: The impact of glycosylation on the pharmacokinetics and effector functions of therapeutic IgG1 monoclonal antibodies has been previously reviewed (Putnam et al. 2010).
3. *Susceptibility to proteolysis*: Gillies and coworkers improved the circulating half-life of antibody-interleukin 2 immunocytokine by two-fold compared with wild type (1.0 h versus 0.54 h) by increasing the resistance to intracellular degradation (Gillies et al. 2002).
4. *Charge*: Deliberate modification of the isoelectric point (pI) of an antibody by approximately one pI unit or more can lead to noticeable differences in the PK of an intact antibody (Igawa et al. 2010; Li et al. 2014; Bumbaca Yadav et al. 2015). Using a humanized anti-IL-6 receptor IgG1 as an example, Igawa et al. showed that lowering the pI point from 9.2 to 7.2 by engineering the V region reduced the IgG elimination in cynomolgus monkeys (Igawa et al. 2010). In contrast, minor changes in the nature of ionic charge resulting in pI differences of less than approximately one pI unit are not expected to affect the biological function of MABs, including tissue retention and whole blood clearance (Boswell et al. 2010b; Khawli et al. 2010).
5. *Effector function*: Effector functions, such as interactions with FcγR, can also regulate elimination and PK of MABs (Mahmood and Green 2005). Mutation of the binding site of FcγR, for example, had dramatic effects on the clearance of an Ab-IL-2 fusion protein (Gillies et al. 1999).
6. *Concomitant medications*: Methotrexate reduced adalimumab apparent CL after single dose and multiple dosing by 29 and 44%, respectively, in patients with RA (Humira (Adalimumab) Prescribing Information 2007). In addition, azathioprine and mycophenolate mofetil were reported to reduce CL of basiliximab by approximately 22 and 51%, respectively (Simulect (Basiliximab) Prescribing Information 2005). The effects of small molecule drugs on the expression of Fcγ receptors could explain this finding. It has also been shown that methotrexate affects expression of FcγRI on monocytes significantly in RA patients (Bunescu et al. 2004).
7. *Off-target binding*: Although specificity to their targets is a major characteristic of MABs, they may have off-target binding that may result in atypical PK, such as faster CL and larger volume distribution. An anti-respiratory syncytial virus MAB, A4b4, developed by affinity maturation of palivizumab, had poor PK in rats and cynomolgus monkeys due to broad nonspecific tissue binding and sequestration (Wu et al. 2007). The rapid elimination of a humanized anti-human amyloid beta peptide MAB, anti-Aβ Ab2, in cynomolgus monkeys was linked to off-target binding to cynomolgus monkey fibrinogen (Vugmeyster et al. 2011). In addition, a humanized anti-fibroblast growth factor receptor 4 MAB had rapid CL in mice that was attributable to binding to mouse complement component 3 (Bumbaca et al. 2011). Other examples of MABs with off-target effects include MABs targeting Factor IXa/X (Sampei et al. 2013), interleukin-21 receptor (Vugmeyster et al. 2010). It is important to eliminate MABs with higher risk of failure at the discovery stage, to increase the success rate. As PK of these therapeutic proteins might be influenced by a large number of both specific and nonspecific factors, Dostalek et al. have proposed multiple pharmacokinetic de-risking tools for selection of MAB lead candidates (Dostalek et al. 2017).
8. *Body weight, age, disease state, and other demographic factors*: Individual characteristics can also change MAB PK (Mould and Sweeney 2007; Ryman and Meibohm 2017) (see Population Pharmacokinetics section).
9. *Albumin*: Albumin is often an indicator of disease status and a significant covariate affecting clearance for several MABs, including infliximab, pertuzumab, trastuzumab emtansine (Lu et al. 2014), and bevacizumab (Dirks and Meibohm 2010). It is believed that albumin, which binds to FcRn at different sites than IgG, is an indicator of increased number of FcRn (Dirks and Meibohm 2010; Fasanmade et al. 2010). Nevertheless, the correlation between the levels of albumin and the CL of pertuzumab and bevacizumab was moderate and dose modification was not recommended (Dirks and Meibohm 2010). Regardless, it has been suggested that serum albumin levels are a predictive factor for PK of infliximab and clinical response to the drug in patients with ulcerative colitis (Fasanmade et al. 2010).
10. *Disease state*: It has been reported that disease state can impact MAB PK. Lower exposure and faster CL for trastuzumab (Yang et al. 2013; Han et al.

2014), bevacizumab (Han et al. 2014), pertuzumab (Kang et al. 2013), and trastuzumab emtansine (Chen et al. 2017) in patients with gastric cancer (GC) versus breast cancer (BC) have been reported. Steady-state trastuzumab trough concentration (C_{trough}) in patients with metastatic GC is 24–63% lower than in BC (Yang et al. 2013). The underlying mechanism for faster CL of MABs in GC is unknown and warrants further research. Population PK analyses of ofatumumab were performed for various diseases with varying CD20 B-cell counts and indicated that target-mediated CL in CLL is greater than that in RA and FL, which is consistent with the higher B-cell count seen in CLL (Struemper et al. 2014). Diabetic comorbidity resulted in 28.7% higher CL/F for ustekinumab (Zhu et al. 2009). Infliximab CL is 40–50% higher in inflammatory bowel disease patients, which is likely due to protein losing enteropathy (Fasanmade et al. 2009). Recently, it has been observed that MABs in immune-oncology, such as pembrolizumab (Li et al. 2017) and nivolumab (Bajaj et al. 2017), have time-dependent CL. Sicker patients tend to have faster CL.

In summary, the association between baseline disease factors and PK complicates the interpretation of the exposure-efficacy analyses for MABs and ADCs in cancer patients, as only one-dose level is usually tested in the pivotal study. Although correction methods can be applied, the effect of disease severity on treatment exposure may result in an over-estimation of exposure–response relationships, i.e. visually a steep trend is seen when the true relationship is flat (Liu et al. 2015; Wang 2016).

THERAPEUTIC MAB–DRUG INTERACTIONS

MABs and other therapeutic proteins are increasingly combined with small molecule drugs to treat various diseases. Assessment of the potential for PK- and/or PD-based MAB–drug interactions is frequently incorporated into the drug development process (Girish et al. 2011). The exposure and response of concomitantly administered drugs can be altered by MABs (MAB as perpetrator), and other drugs can effect the PK and PD of therapeutic MABs (MAB as victim).

Several different mechanisms have been proposed for MAB–drug interactions. Various cytokines and cytokine modulators can influence the expression and activity of cytochrome P450 (CYP) enzymes and drug transporters (Lee et al. 2010). Therefore, if a therapeutic MAB is a cytokine or cytokine modulator, it can potentially alter the systemic exposure and/or clinical response of concomitantly administered drugs that are substrates of CYPs or transporters (Huang et al. 2010), particularly those with narrow therapeutic windows. For example, an increase in cyclosporin A (CsA) trough level was observed when given in combination with muromonab (Vasquez and Pollak 1997). Similarly, basiliximab has been shown to increase CsA and tacrolimus level when used in combination (Sifontis et al. 2002). In diseases states such as infection or inflammation, cytokines or cytokine modulators can also normalize previously changed activity of CYPs or transporters, thereby altering the exposure of coadministered drugs. Examples include tocilizumab coadministered with omeprazole and tocilizumab coadministered with simvastatin. At present, in vitro and preclinical systems have shown limited value in predicting a clinically relevant effect of cytokine-mediated therapeutic protein (TP)-DDI, and clinical evidence is preferred for informing the evolving risk assessment for TP-DDI (Huang et al. 2010; Slatter et al. 2013). To determine the necessity for a dedicated clinical DDI study, a four-step approach was proposed by the IQ Consortium/FDA TP-DDI workshop (San Diego 2012) in assessing TP-DDI risk for cytokines or cytokine modulators on CYP enzymes. This includes stepwise investigations of: (1) the disease effect on cytokine levels and CYP expression; (2) TP mechanism and its impact on cytokine-mediated DDI; (3) DDI liability of the concurrently used small molecule drugs; and (4) the above overall driving force in determining appropriate clinical TP-DDI strategies (Kenny et al. 2013). To date, a few dedicated clinical DDI studies have been performed for MABs that specifically target cytokines or cytokine receptors, e.g., tocilizumab (Schmitt et al. 2011), sirukumab (Zhuang et al. 2015), daclizumab HYP (Tran et al. 2016), and dupilumab (Davis et al. 2018). However, the overall impact of these cytokine-blocking MABs on PK of the CYP substrates (MAB as a perpetrator) were minimal (no effect, e.g., daclizumab HYP, ustekinumab, and dupilumab) or moderate (18–57% reduction in AUC for CYP 2C19 or 3A4 substrates, e.g., tocilizumab and sirukumab) and have not been implicated in dose justification for the relevant concurrent medicines.

MAB–drug interactions can also occur when a therapeutic MAB is administered with a concomitant drug that can alter the formation of ADAs. This may in turn alter MAB clearance from the systemic circulation. For example, methotrexate (MTX) reduced the apparent CL of adalimumab by 29 and 44% after single and repeated dosing (Humira (Adalimumab) Prescribing Information 2007). MTX also had similar effect on infliximab (Maini et al. 1998). PD-based interactions can result from alteration of target biology, such as the site of expression, relative abundance of expression, and the pharmacology of the target (Girish et al. 2011). Examples include efalizumab in combination with

triple immune-suppressant therapy (Vincenti et al. 2007) and anakinra in combination with etanercept (Genovese et al. 2004).

To date, evidence of therapeutic MAB–drug interactions via nonspecific clearance appears to be limited, although down-regulation of Fcγ receptors by MTX is observed in patients with RA. It is possible that changes in Fcγ receptors can affect MAB clearance in the presence of MTX (Girish et al. 2011).

ADCs can also interact with drugs or MABs via the mechanisms described above. However, evidence of ADC–drug or ADC–MAB interaction appears to be absent. Lu et al. reported lack of interaction between trastuzumab emtansine (T-DM1) and pertuzumab in patients with HER2-positive metastatic breast cancer (Lu et al. 2012). Similarly, no interaction was observed between T-DM1 and paclitaxel or T-DM1 and docetaxel (Lu et al. 2012). With the theoretical potential for, and current experiences with, MAB–drug interactions, a question and risk-based integrated approach depending on the mechanism of the MABs and patient population have been progressively adopted during drug development to address important questions regarding the safety and efficacy of MAB and drug combinations (Girish et al. 2011). Various in vitro test systems have been used to provide some insight into the MAB–drug interactions, such as isolated hepatocytes and liver microsomes. However, the interpretation of these in vitro data is difficult. More importantly, prospective predictions of drug interactions based on in vitro findings have not been feasible for MABs. Therefore, clinical methods are primarily used to assess MAB–drug interactions. Three common methods used are population PK, clinical cocktail studies, and less frequently, dedicated drug interaction studies. Details of various strategies used in pharmaceutical industry were reviewed in a 2011 AAPS white paper (Girish et al. 2011). Recently, PBPK modeling has been used as a tool to predict drug interactions for antibody-drug conjugates (Chen et al. 2015).

PREDICTION OF HUMAN PK/PD BASED ON PRECLINICAL INFORMATION

Prior to a first-in-human (FIH) clinical study, a number of preclinical in vivo and in vitro experiments are conducted to evaluate the PK/PD, safety, and efficacy of a new drug candidate. However, the ultimate goal is at all times to predict how these preclinical results on PK, safety, and efficacy data translate into a given patient population. Therefore, the objective of translational research is to predict PK/PD/safety outcomes in a target patient population, acknowledging the similarities and differences between preclinical and clinical settings.

Over the years, many theories and approaches have been proposed and used for scaling preclinical PK data to humans (Fig. 8.9). Allometric scaling, based on a power–law relationship between size of the body and physiological and anatomical parameters, is the simplest and most widely used approach (Dedrick 1973; Mahmood 2005, 2009). More recently, experimental efforts have been dedicated to accurate measurement of physiological parameters that are required for calculating drug concentrations at site of action and for physiologically based models (Boswell et al. 2010a, 2012, 2014). Physiologically based PK modeling (Shah and Betts 2012), species-invariant time method (Dedrick approach) (Oitate et al. 2011), and nonlinear mixed effect modeling based on allometry (Jolling et al. 2005; Martin-Jimenez and Riviere 2002) have also been used for interspecies scaling of PK. While no single scaling method has been shown to definitively predict human PK in all cases, especially for small molecule drugs (Tang and Mayersohn 2005), the PK for MABs can be predicted reasonably well, especially for MAB at doses where the dominant clearance route is likely to be independent of concentration. Most therapeutic MABs bind to nonhuman primate antigens more often than to rodent antigens, due to the greater sequence homology observed between nonhuman primates and humans. The binding epitope, in vitro binding affinity to antigen, binding affinity to FcRn, tissue cross-reactivity profiles, and disposition and elimination pathways of MABs are often comparable in nonhuman primates and humans. It has recently been demonstrated that clearance and distribution volume of MABs with linear PK in humans can be reasonably projected based on data from nonhuman primates alone, with a fixed scaling exponent ranging from 0.75 to 0.9 for CL and a fixed scaling exponent 1 for volume of distribution (Oitate et al. 2011; Ling et al. 2009; Wang and Prueksaritanont 2010; Deng et al. 2011; Dong et al. 2011). For MABs that exhibited nonlinear PK, the best predictive performance was obtained above doses that saturated the target of the MAB (Dong et al. 2011). Pharmacokinetic prediction for low doses of a MAB with nonlinear elimination remains challenging and will likely require further exploration of species difference in target expression level, target antibody binding and target kinetics, as well as strategic in vivo animal PK studies, designed with relevant dose ranges. Immunogenicity is an additional challenge for the prediction of MAB PK. Alterations in the PK profile due to immune-mediated clearance mechanisms in preclinical species cannot be scaled up to humans, since animal models are not predictive of human immune response to human MABs. Thus, either excluding ADA-positive animals from PK scaling

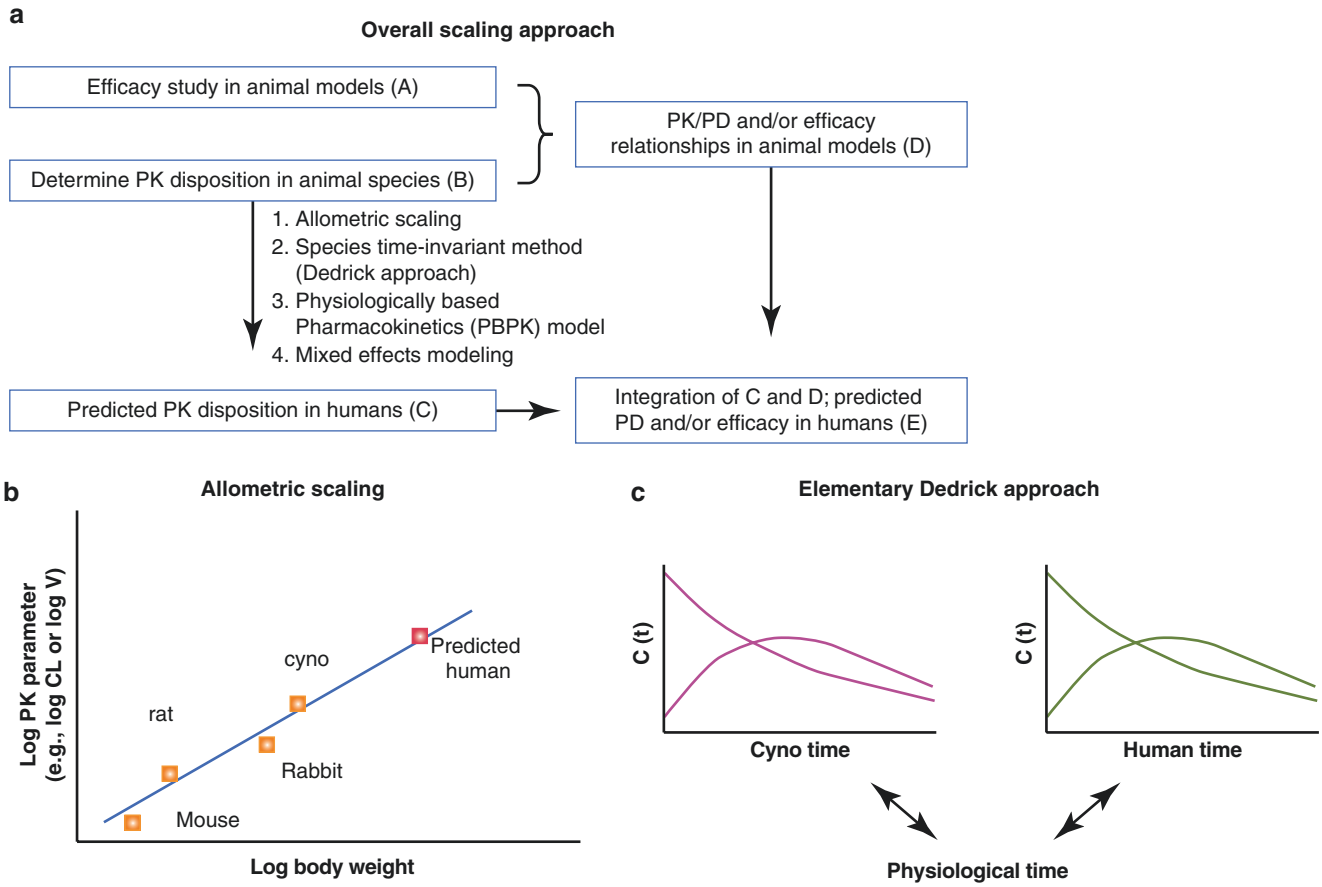

Figure 8.9 ■ PK/PD scaling approach from preclinical studies to humans. (**a**) Overall scaling approach. (**b**) Allometric scaling. (**c**) Elementary Dedrick approach

analysis or using only the early time points prior to ADAs observation in ADA-positive animals has been a standard practice in the industry.

Due to its complexity, any extrapolation of PD to humans requires more thorough consideration than for PK. Little is known about allometric relationships in PD parameters. It is expected that the physiological turnover rate constants of most general structures and functions among species should obey allometric principles, whereas capacity and sensitivity tend to be similar across species (Mager et al. 2009). Through integration of PK/PD modeling and interspecies scaling, PD effects in humans may be predicted if the PK/PD relationship is assumed to be similar between animal models and humans (Duconge et al. 2004; Kagan et al. 2010). For example, a PK/PD model was first developed to optimize the dosing regimen of a MAB against EGF/r3 using tumor-bearing nude mice as an animal model of human disease (Duconge et al. 2004). This PK/PD model was subsequently integrated with allometric scaling to calculate the dosing schedule required in a potential clinical trial to achieve a specific effect (Duconge et al. 2004).

In summary, species differences in antigen expression level, antigen–antibody binding and antigen kinetics, differences in FcRn binding between species, the immunogenicity, and other factors must be considered during PK/PD scaling of a MAB from animals to humans.

ROLE OF PK/PD IN CLINICAL DEVELOPMENT OF ANTIBODY THERAPEUTICS

Drug development has traditionally been performed in sequential phases, divided into preclinical as well as clinical phases I–IV. During the development phases of the molecules, the safety and PK/PD characteristics are established in order to select a compound for development and define a dosing regimen. This information-gathering process has been characterized as two successive learning–confirming cycles (Sheiner and Wakefield 1999; Sheiner 1997).

The first cycle (phases I and IIa) comprises learning about the dose regimen that is tolerated in healthy subjects and confirming that this dose regimen has shown drug-target engagement, acceptable tolerability

and measurable clinical benefits in the targeted patients. An affirmative answer at this first cycle provides the justification for a larger and more costly second learn–confirm cycle (phases IIb and III), where the learning step is focused on defining the drug benefit/risk profile, whereas the confirm step is aimed at demonstrating acceptable benefit/risk in a large patient population (Meibohm and Derendorf 2002).

The drug development process at the clinical stage provides several opportunities for integration of PK/PD concepts. Clinical phase I dose escalation studies provide, from a PK/PD standpoint, the unique opportunity to evaluate the dose–concentration–effect relationship for therapeutic and toxic effects over a wide range of doses up to or even beyond the maximum tolerated dose under controlled conditions (Meredith et al. 1991). PK/PD evaluations at this stage of drug development can provide crucial information regarding the potency and tolerability of the drug in vivo and the verification and suitability of the PK/PD relationship established during preclinical studies.

Collecting robust data on the PK of the drug and PD or disease biomarkers that are indicative of drug pharmacology and disease progression/improvement is key to informing dose selection. Tocilizumab, omalizumab, and evolocumab are examples of MABs that utilized PK/PD or disease biomarker data to facilitate dose selection for pivotal trials, final doses and/or label revisions. In general, the strategy includes (1) understanding the PK profile and selecting clinical doses in the linear range, if possible; (2) identifying biomarkers having profiles correlated to clinically meaningful endpoints for PK/PD or exposure-response analyses, and (3) leveraging modeling and simulation approaches to predict the clinical outcome under different regimen scenarios, which is essential to determine the dose regimen for a pivotal trial or the final dose regimen on the label.

In the case of omalizumab, a dosing table for asthma patients was developed to select the dose based on an individual's pre-treatment serum IgE level and body weight. The dosing table was designed to achieve a serum-free IgE level associated with clinical improvement (Hochhaus et al. 2003). PK/PD modeling and simulation approaches were subsequently used to revise and expand the dosing table (Lowe et al. 2015; Honma et al. 2016). In the case of evolocumab, a high-level summary of the development program and dosing strategy follows.

Evolocumab is a recombinant, human IgG2 MAB that specifically binds to human proprotein convertase subtilisin/kexin type 9 (PCSK9). It prevents PCSK9 from interacting with the low density lipoprotein receptor (LDLR), thus upregulating LDLR, increasing uptake of circulating LDL-cholesterol (LDL-C) and reducing LDL-C concentration in plasma (Page and Watts 2015). Evolocumab is used as an adjunct to diet and maximally tolerated statin therapy for the treatment of adults with heterozygous familial hypercholesterolemia or clinical atherosclerotic cardiovascular disease. Its use is also indicated as an adjunct to diet and other LDL-lowering therapies for the treatment of patients with homozygous familial hypercholesterolemia.

The PK of evolocumab following multiple SC doses was evaluated in a Phase 1 study in subjects on a stable dose of statin over a dose range of 14–420 mg of evolocumab weekly, every 2 weeks, or every 4 weeks. Multiple doses of evolocumab resulted in nonlinear PK for the lower doses (up to 140 mg SC). Dose regimens of 140 mg and greater led to linear PK and concentrations associated with near complete suppression of PCSK9 (CDER 2014). Dose-dependent decreases in LDL-C levels were seen following treatment with evolocumab (CDER 2014) and this PD readout is also indicative of a meaningful clinical readout. There was a clear exposure-response relationship between evolocumab trough concentrations and LDL-C response (CDER 2014). These PK/PD data and the exposure-response relationship were used to support the final approved dose and dosing regimen.

■ Efalizumab Case Study (Raptiva®)

In the following sections, the recombinant humanized IgG1 MAB efalizumab is provided as a more detailed case study to understand the various steps during the development of therapeutic antibodies for various indications. Raptiva® received approval for the treatment of patients with psoriasis in more than 30 countries, including the United States and the European Union (Raptiva (Efalizumab) [Prescribing Information] 2004). However, it was withdrawn from the market when the use of efalizumab was found to be associated with an increased risk of progressive multifocal leukoencephalopathy (PML).

A summary of the preclinical program, the overall PK/PD data from multiple clinical studies, and the selection of the subcutaneous doses of efalizumab for the treatment of psoriasis will be discussed. Psoriasis is a chronic skin disease characterized by abnormal keratinocyte differentiation and hyperproliferation and by an aberrant inflammatory process in the dermis and epidermis. T cell infiltration and activation in the skin and subsequent T cell-mediated processes have been implicated in the pathogenesis of psoriasis (Krueger 2002). Efalizumab is a targeted inhibitor of T cell interactions (Werther et al. 1996). An extensive preclinical research program was conducted to study the safety and MOA of efalizumab. Multiple clinical studies were also conducted to investigate the efficacy, safety, PK, PD, and MOA of efalizumab in patients with psoriasis.

Preclinical Program of Efalizumab

A thorough and rigorous preclinical program provides a linkage between drug discovery and clinical development. At the preclinical stage, activities may include the evaluation of in vivo potency and intrinsic activity, the identification of bio-/surrogate markers, understanding of MOA, and characterization of nonclinical PK/PD, as well as dosage form/regimen selection and optimization. The role of surrogate molecules in assessing ADME of therapeutic antibodies is important as the antigen specificity of humanized MABs limits their utility in studies with rodents. Surrogate rodent MABs (mouse/rat) provide a means of gaining knowledge of PK and PD in a preclinical rodent model, facilitating dose optimization in the clinic.

In the case of efalizumab, to complete a more comprehensive safety assessment, a chimeric rat antimouse CD11a antibody, muM17, was developed and evaluated as a species-specific surrogate molecule for efalizumab. muM17 binds mouse CD11a with specificity and affinity similar to that of efalizumab to its human target antigen. In addition, pharmacological activities of muM17 in mice were demonstrated to be similar to those of efalizumab in humans (Clarke et al. 2004; Nakakura et al. 1993).

The preclinical ADME program for efalizumab consisted of PK, PD (CD11a down-modulation and saturation), and toxicokinetic data from PK, PD, and toxicology studies with efalizumab in chimpanzees and with muM17 in mice. The use of efalizumab in the chimpanzee and muM17 in mice for PK and PD and safety studies was supported by in vitro activity assessments. The preclinical data were used for PK and PD characterization, PD-based dose selection, and toxicokinetic support for confirming exposure in toxicology studies. Together, these data supported both the design of the preclinical program and its relevance to the clinical program.

The observed PD as well as the MOA of efalizumab and muM17 is attributed to binding CD11a present on cells and tissues. The binding affinities of efalizumab to human and chimpanzee CD11a on CD3 lymphocytes are comparable, supporting the use of chimpanzees as a preclinical model for human responses. CD11a expression has been observed to be greatly reduced on T lymphocytes in chimpanzees and mice treated with efalizumab and muM17, respectively. Expression of CD11a is restored as efalizumab and muM17 are eliminated from the plasma.

The disposition of efalizumab and of the mouse surrogate muM17 is mainly determined by the combination of both specific interactions with the ligand CD11a and by their IgG1 framework. The disposition is governed by the species specificity of the antibody for its ligand CD11a, the amount of CD11a in the system, and the administered dose. Binding to CD11a serves as a major pathway for clearance of these molecules, which leads to nonlinear PK depending on the relative amounts of CD11a and efalizumab or muM17 (Coffey et al. 2005).

Based on the safety studies, efalizumab was considered to be generally well tolerated in chimpanzees at doses up to 40 mg/kg/week IV for 6 months, providing an exposure ratio of 339-fold based on cumulative dose and 174-fold based on the cumulative AUC, compared with a clinical dose of 1 mg/kg/week. The surrogate antibody muM17 was also well tolerated in mice at doses up to 30 mg/kg/week SC. Overall, efalizumab was considered to have an excellent nonclinical safety profile, thereby supporting the use in adult patients. There was no signal for PML in the nonclinical studies, which subsequently led to withdrawal of efalizumab from the market.

Clinical Program of Efalizumab: PK/PD Studies, Assessment of Dose, Route, and Regimen

Efalizumab PK and PD data were available from ten studies in which more than 1700 patients with psoriasis received IV or SC efalizumab. In the phase I studies, PK and PD parameters were characterized by extensive sampling during treatment; in the phase III trials, steady-state trough levels were measured once or twice during the first 12-week treatment period for all the studies and during extended treatment periods for some studies. Several early phase I and II trials examined IV injection of efalizumab, and dose-ranging findings from these trials served as the basis for SC dosing levels used in several subsequent phase I and all phase III trials.

IV Administration of Efalizumab

The PK of MABs varies greatly, depending primarily on their affinity for and the distribution of their target antigen (Lobo et al. 2004). Efalizumab exhibited concentration-dependent nonlinear PK after administration of single IV doses of 0.03, 0.1, 0.3, 0.6, 1.0, 2.0, 3.0, and 10.0 mg/kg in a phase I study. This nonlinearity is directly related to specific and saturable binding of efalizumab to its cell surface receptor, CD11a, and has been described by a PK/PD model developed by Bauer et al. (1999), which was expanded to a PK/PD/efficacy model by Ng et al. (2005). The PK profiles of efalizumab following single IV doses with observed data and model predicted fit are presented in Fig. 8.10. Mean CL decreased from 380 to 6.6 mL/kg/day for doses of 0.03 mg/kg to 10 mg/kg, respectively. The volume of distribution of the central compartment

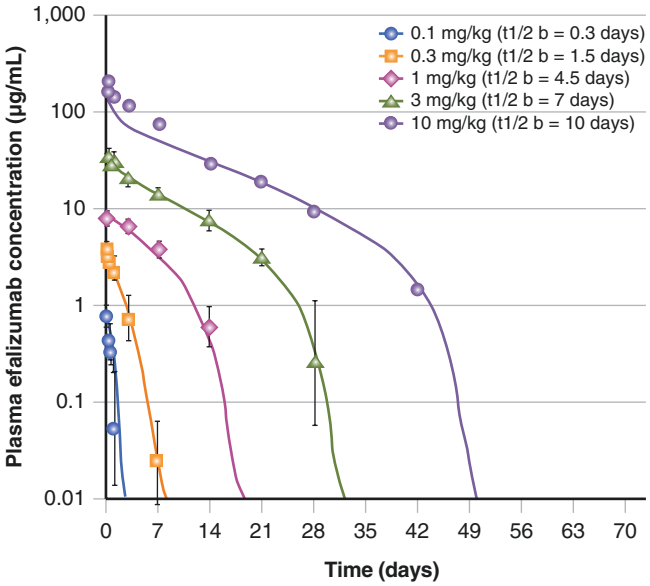

Figure 8.10 ■ Plasma concentration versus time profile for efalizumab following single IV doses in psoriasis patients (Ng et al. 2005)

(Vc) of efalizumab was 110 mL/kg at 0.03 mg/kg (approximately twice the plasma volume) and decreased to 58 mL/kg at 10 mg/kg (approximately equal to plasma volume), consistent with saturable binding of efalizumab to CD11a in the vascular compartment. Because of efalizumab's nonlinear PK, its half-life ($t_{1/2}$) is dose dependent.

In a phase II study of efalizumab, it was shown that at a weekly dosage of 0.1 mg/kg IV, patients did not maintain maximal down-modulation of CD11a expression and did not maintain maximal saturation. Also, at the end of 8 weeks of efalizumab treatment, 0.1 mg/kg/week IV, patients did not have statistically significant histological improvement and did not achieve a full clinical response. The minimum weekly IV dosage of efalizumab tested that produced histological improvements in skin biopsies was 0.3 mg/kg/week. This dosage resulted in submaximal saturation of CD11a binding sites but maximal down-modulation of CD11a expression. Improvements in patients' psoriasis were also observed, as determined by histology and by the Psoriasis Area and Severity Index (PASI) (Papp et al. 2001).

Determination of SC Doses

Although efficacy was observed in phase I and II studies with 0.3 mg/kg/week IV efalizumab, dosages of 0.6 mg/kg/week and greater (given for 7–12 weeks) provided more consistent T lymphocyte CD11a saturation and maximal PD effect. At dosages ≤0.3 mg/kg/week, large between-subject variability was observed, whereas at dosages of 0.6 or 1.0 mg/kg/week, patients experienced better improvement in PASI scores, with lower between-patient variability in CD11a saturation and down-modulation. Therefore, since the desired route of administration was SC, this IV dosage was used to estimate an appropriate minimum SC dose of 1 mg/kg/week (based on a 50% bioavailability) that would induce similar changes in PASI, PD measures, and histology. The safety, PK, and PD of a range of SC efalizumab doses (0.5–4.0 mg/kg/week administered for 8–12 weeks) were evaluated initially in two phase I studies (Gottlieb et al. 2003). To establish whether a higher SC dosage might produce better results, several phase III clinical trials assessed a 2.0 mg/kg/week SC dosage in addition to the 1.0 mg/kg/week dosage. A dose of 1.0 mg/kg/week SC efalizumab was selected as it produced sufficient trough levels in patients to maintain the maximal down-modulation of CD11a expression and binding-site saturation between weekly doses (Joshi et al. 2006). Figure 8.11 depicts the serum efalizumab levels, CD11a expression, and available CD11a binding sites on T lymphocytes (mean ± SD) after SC administration of 1 mg/kg efalizumab.

SC Administration of Efalizumab

The PK of SC efalizumab was well characterized following multiple SC doses of 1.0 and 2.0 mg/kg/week (Joshi et al. 2006; Mortensen et al. 2005). A phase I study that collected steady-state PK and PD data for 12 weekly SC doses of 1.0 and 2.0 mg/kg in psoriasis patients provided most of the pharmacologic data relevant to the product that was on the market prior to its withdrawal. Although peak serum concentration after the last dose (C_{max}) was observed to be higher for the 2.0 mg/kg/week (30.9 µg/mL) than for the 1.0 mg/kg/week dosage (12.4 µg/mL), no additional changes in PD effects were observed at the higher dosages (Mortensen et al. 2005). Following a dose of 1.0 mg/kg/week, serum efalizumab concentrations were adequate to induce maximal down-modulation of CD11a expression and a reduction in free CD11a binding sites on T lymphocytes (Fig. 8.12). Steady-state serum efalizumab levels were reached more quickly with the 1.0 mg/kg/week dosage at 4 weeks compared with the 2.0 mg/kg/week dosage at 8 weeks (Mortensen et al. 2005), which is in agreement with the average effective $t_{1/2}$ of 5.5 days for SC efalizumab 1.0 mg/kg/week (Boxenbaum and Battle 1995). The bioavailability was estimated at approximately 50%. Population PK analyses indicated that body weight was the most significant covariate affecting efalizumab SC clearance, thus supporting body weight-based dosing for efalizumab (Sun et al. 2005).

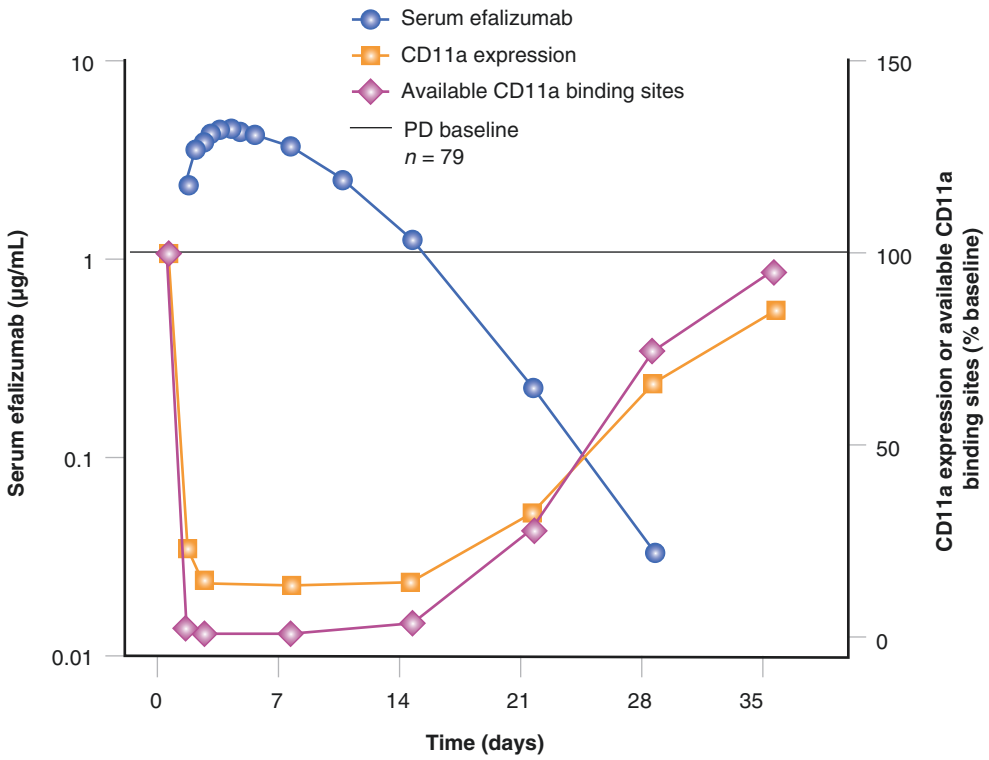

Figure 8.11 ■ PK/PD profile following efalizumab in humans (1 mg/kg SC) (Joshi et al. 2006)

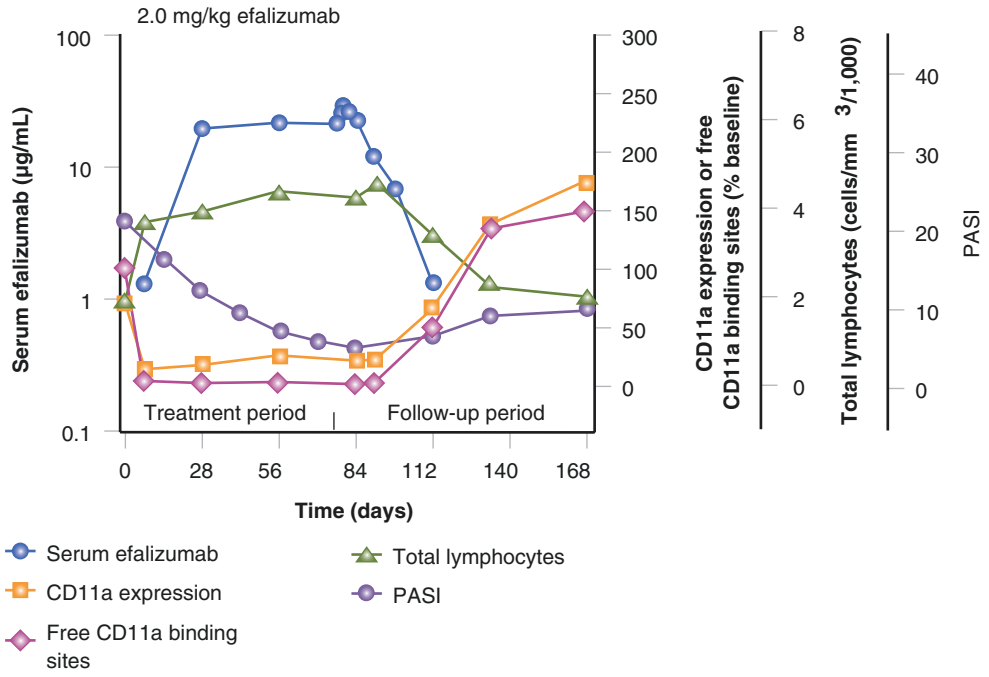

Figure 8.12 ■ Serum efalizumab, CD11a expression, and free CD11a binding sites on T lymphocytes, absolute lymphocyte counts, and Psoriasis Area and Severity Index (PASI) score (mean) following 1.0 mg/kg/week SC efalizumab for 12 weeks and 12 weeks post-treatment (Mortensen et al. 2005)

POPULATION PHARMACOKINETICS OF MONOCLONAL ANTIBODIES

Compared to many small molecule drugs, MABs typically exhibit less inter- and intra-subject variability of the standard PK parameters such as volume of distribution and clearance. However, it is possible that certain pathophysiological conditions may result into substantially increased intra- and inter-patient variability. In addition, patients are usually not very homogeneous; patients vary in sex, age, body weight; they may have concomitant disease and may be receiving multiple drug treatments. Even the diet, lifestyle,

ethnicity, and geographic location can differ from a selected group of "normal" subjects. These covariates can have substantial influence on PK parameters. Therefore, good therapeutic practice should always be based on an understanding of both the influence of covariates on PK parameters as well as the PK variability in a given patient population. With this knowledge, dosage adjustments can be made to accommodate differences in PK due to genetic, environmental, physiological, or pathological factors, for instance, in case of compounds with a relatively small therapeutic index. The framework of application of population PK during drug development is summarized in the FDA guidance document entitled "Guidance for Industry—Population Pharmacokinetics" (FDA 1999).

For population PK data analysis, there are generally two reliable and practical approaches. One approach is the standard two-stage (STS) method, which estimates parameters from the plasma drug concentration data for an individual subject during the first stage. The estimates from all subjects are then combined to obtain a population mean and variability estimates for the parameters of interest. The method works well when sufficient drug concentration-time data are available for each individual patient; typically these data are gathered in phase 1 clinical trials. A second approach, nonlinear mixed effect modeling (NONMEM), attempts to fit the data and partition the differences between theoretical and observed values into random error terms. The influence of fixed effect (i.e., age, sex, body weight) can be identified through a regression model building process.

The original scope for the NONMEM approach was its applicability even when the amount of time-concentration data obtained from each individual is sparse and conventional compartmental PK analyses are not feasible. This is usually the case during the routine visits in phase III or IV clinical studies. Nowadays the NONMEM approach is applied far beyond its original scope due to its flexibility and robustness. It has been used to describe data-rich phase I and phase IIa studies or even preclinical data to guide and expedite drug development from early preclinical to clinical studies (Aarons et al. 2001; Chien et al. 2005).

There has been increasing interest in the use of population PK and PD analyses for different antibody products (i.e. antibodies, antibody fragments, or antibody fusion proteins) over the past 15 years (Dirks and Meibohm 2010; Agoram et al. 2007; Gibiansky and Frey 2012; Gibiansky and Gibiansky 2009; Nestorov et al. 2004; Zheng et al. 2011; Zhou et al. 2004; Yim et al. 2005; Hayashi et al. 2007; Lee et al. 2003). One example involving analysis of population plasma concentration data involved a dimeric fusion protein, etanercept. A one-compartment first-order absorption and elimination population PK model with interindividual and inter-occasion variability on CL, volume of distribution, and absorption rate constant, with covariates of sex and race on apparent CL and body weight on CL and volume of distribution, was developed for etanercept in rheumatoid arthritis adult patients (Lee et al. 2003). The population PK model for etanercept was further applied to pediatric patients with juvenile RA and established the basis of the 0.8 mg/kg once weekly regimen in pediatric patients with juvenile RA (Yim et al. 2005). Unaltered etanercept PK with concurrent methotrexate in patients with RA has been demonstrated in a phase IIIb study using a population PK modeling approach (Zhou et al. 2004). Thus, no etanercept dose adjustment is needed for patients taking concurrent MTX. A simulation exercise of using the final population PK model of subcutaneously administered etanercept in patients with psoriasis indicated that the two different dosing regimens (50 mg QWk versus 25 mg BIWk) provide a similar steady-state exposure (Nestorov et al. 2004). Therefore, their respective efficacy and safety profiles are likely to be similar as well.

An added feature is the development of a population model involving both PK and PD. Population PK/PD modeling has been used to characterize drug PK and PD with models ranging from simple empirical PK/PD models to advanced mechanistic models by using drug–receptor binding principles or other physiologically based principles. A mechanism-based population PK and PD binding model was developed for a recombinant DNA-derived humanized IgG1 MAB, omalizumab (Hayashi et al. 2007). Clearance and volume of distribution for omalizumab varied with body weight, whereas CL and rate of production of IgE were predicted accurately by baseline IgE, and overall, these covariates explained much of the interindividual variability. Furthermore, this mechanism-based population PK/PD model enabled the estimation of not only omalizumab disposition but also the binding with its target, IgE, and the rate of production, distribution, and elimination of IgE.

Recently, a platform population PK approach has been used to characterize MAB PK to improve the efficiency of study design, such as optimal dose regimens and PK sampling times. Davda et al. (2014) determined typical population PK values for four MABs with linear elimination using model-based meta-analysis, which can be utilized to prospectively optimize FIH study designs. A platform model describing PK properties of vc-MMAE antibody-drug conjugates based on 8 ADCs is reported by Kagedal et al. (2017). The model could be applied to predict PK-profiles of future vc-MMAE ADCs, estimate individual exposure for the subsequent exposure-response analysis, and optimize study design.

Population PK/PD analysis can capture uncertainty and the expected variability in PK/PD data generated in preclinical studies or early phases of clinical development. Understanding the associated PK or PD variability and performing clinical trial simulation by incorporating the uncertainty from the existing PK/PD data allows projecting a plausible range of doses for future clinical studies and final practical uses.

FUTURE PERSPECTIVE

The success of MABs as new therapeutic agents in several disease areas such as oncology, inflammatory diseases, autoimmune diseases, and transplantation has triggered growing scientific, therapeutic, and business interest in the MAB technology. The market for therapeutic MABs is one of the most dynamic sectors within the pharmaceutical industry. Further growth is expected by developing MABs towards other surface protein targets, which are not covered yet by marketed MABs. Particularly, the technological advancement in the area of ADCs and MAB fragments may overcome some of the limitations of MABs by providing highly potent drugs selectively to target compartments and to extend the distribution of the active moiety, which are typically not reached by MABs. ADCs hold great promise for selective drug delivery of potent drugs with unfavorable own selectivity to target cells (e.g., highly potent cytotoxic drugs). Several of such ADCs are under development to target different tumor types and are expected to reach the market in the next several years. Modification of the MAB structure allows adjusting the properties according to therapeutic needs (e.g., adjusting half-life, increasing volume of distribution, changing clearance pathways). By using modified MAB derivatives, optimized therapeutic agents might become available. For example, this technology has been successfully used for two antibody fragments marketed in inflammatory disease and anti-angiogenesis (abciximab, ranibizumab).

Bispecific antibodies represent another promising new methodological approach to antibody therapy. Technological refinements in antibody engineering have allowed the production of bispecific antibodies that are simultaneously directed towards two distinct target antigens (Holmes 2011). For instance, the CDR consisting of the variable domains (V_L and V_H) at the tip of one arm of an IgG may be asymmetrically designed to bind to a different target than that of the other arm (Fig. 8.1). Symmetrical formats in which each arm can bind two targets are also possible.

MABs have become a key part of the pharmaceutical armamentarium, especially in the oncology and immunology settings and will continue to be a focus area for drug discovery and development. More specifically, the recent approvals of MABs like pembrolizumab, nivolumab and atezolizumab in cancer immunotherapy have revolutionized cancer treatment paradigm. These MABs, either as monotherapy or in combinations with other cancer immunotherapies, including cancer vaccines, bispecifics and other modalities, offer tremendous promise for personalized medicine.

SELF-ASSESSMENT QUESTIONS

Questions

1. What are the structural differences among the five immunoglobulin classes?
2. What are key differences in PK/PD between MABs and small molecule drugs?
3. Why do IgGs typically show nonlinear PK in the lower plasma (serum) concentration range?
4. What is a surrogate MAB and how can it potentially be used in the drug development process of MABs?
5. Which other modes of actions apart from ADCC—antibody dependent cellular cytotoxicity are known for MABs? What are the key steps of ADCC?
6. Why do IgGs have a longer in vivo half-life compared with other Igs?
7. What are the development phases for antibody therapeutics? What major activities are involved in each phase?

Answers

1. The following structural properties distinguish MABs:
   The molecular form varies across the five immunoglobulin classes: IgG, IgD, and IgE are monomers; IgM forms a pentamer or hexamer, and IgA exists either as a monomer or dimer. Consequently, the molecular weights of various Igs differ (IgG 150–169 kD, IgA 160–300 kD, IgD 175 kD, IgE 190, IgM 950 kD).
2. Metabolism of MABs appears to be simpler than for small molecules. In contrast to small molecule drugs, the typical metabolic enzymes and transporter proteins, such as cytochrome P450, multidrug resistance (MDR) efflux pumps, are not involved in the disposition of MABs. Therefore, drug–drug interaction studies for those disposition processes are only part of the standard safety assessment for small molecules and not for MABs.
   MABs, which have a protein structure, are metabolized by proteases. These enzymes are ubiquitously available in mammalian organisms. In contrast, small molecule drugs are primarily metabolized in the liver.

Because of their large molecular weight, intact MABs are typically not cleared via the renal elimination route. However, renal clearance processes can play a major role in the elimination of small molecule drugs.

PK of MABs usually is dependent on the binding to the pharmacological target protein and shows nonlinear behavior as consequence of its saturation kinetics.

In general, MABs have a longer half-life (on the order of days and weeks) than small molecule drugs (typically on the order of hours).

The distribution of MABs is very restricted (volume of distribution in the range of 0.1 L/kg). As a consequence, MABs do have limited access to tissue compartments (e.g., brain) as potential target sites via passive, energy-independent distribution processes only.

3. At lower concentrations, MABs generally show nonlinear PK due to receptor-mediated clearance processes, which are characterized by small capacity of the clearance pathway and high affinity to the target protein. Consequently at these low concentrations, MABs exhibit typically shorter half-life. With increasing doses, these receptors become saturated, and the clearance as well as elimination half-life decreases until it becomes constant. The clearance in the higher concentration range, which is dominated by linear, non target-related clearance processes, is therefore also called nonspecific clearance in contrast to the target-related, specific clearance.
4. A surrogate MAB has similar antigen specificity and affinity in experimental animals (e.g., mice and rats) compared to those of the corresponding human antibody in humans. It is quite common that the antigen specificity limits ADME studies of humanized MABs in rodents. Studies using surrogate antibodies might lead to important information regarding safety, MOA, disposition of the drug, tissue distribution, and receptor pharmacology in the respective animal species, which might be too cumbersome and expensive to be conducted in nonhuman primates. Surrogate MABs (from mouse or rat) provide a means to gain knowledge of ADME and PD in preclinical rodent models and might facilitate the dose selection for clinical studies.
5. Apart from ADCC, MABs can exert pharmacological effects by multiple mechanisms that include direct modulation of the target antigen, complement-dependent cytotoxicity (CDC) and apoptosis. The key steps of ADCC are (1) opsonization of the targeted cells, (2) recognition of antibody-coated targeted cells by Fc receptors on the surface of monocytes, macrophages, natural killer cells, and other cells, and (3) destruction of the opsonized targets by phagocytosis of the opsonized targets and/or by toxic substances released after activation of monocytes, macrophages, natural killer cells, and other cells.
6. IgG can bind to neonatal Fc receptor (FcRn) in the endosome, which protects IgG from catabolism via proteolytic degradation. This protection results into a slower clearance and thus longer plasma half-life of IgGs. Consequently, changing the FcRn affinity allows adjustment of the clearance of MABs (higher affinity—lower clearance), which can be employed to tailor the PK of these molecules.
7. Pre-IND, phase I, II, III, and IV are the major development phases for antibody therapies. Safety pharmacology, toxicokinetics, toxicology, tissue cross-reactivity, local tolerance, PK support for candidate selection, assay support for PK/PD, and PK/PD support for dose/route/regimen are major activities in the pre-IND phase. General toxicity, reproductive toxicity, carcinogenicity, immunogenicity, characterization of dose–concentration–effect relationship, material comparability studies, mechanistic modeling approach, and population PK/predictions are major activities from phase I to phase III. Further studies might be performed as needed after the MAB got market authorization. These studies are called phase IV studies.

Acknowledgments Editorial and technical support was provided by AnshinBiosolutions, Corp.

REFERENCES

Aarons L, Karlsson MO, Mentre F, Rombout F, Steimer JL, van Peer A (2001) Role of modelling and simulation in Phase I drug development. Eur J Pharm Sci 13(2):115–122

Agoram BM, Martin SW, van der Graaf PH (2007) The role of mechanism-based pharmacokinetic-pharmacodynamic (PK-PD) modelling in translational research of biologics. Drug Discov Today 12(23-24):1018–1024. https://doi.org/10.1016/j.drudis.2007.10.002

Albrecht H, DeNardo SJ (2006) Recombinant antibodies: from the laboratory to the clinic. Cancer Biother Radiopharm 21(4):285–304. https://doi.org/10.1089/cbr.2006.21.285

Baert F, Noman M, Vermeire S, Van Assche G, DH G, Carbonez A, Rutgeerts P (2003) Influence of immunogenicity on the long-term efficacy of infliximab in Crohn's disease. N Engl J Med 348(7):601–608

Bajaj G, Wang X, Agrawal S, Gupta M, Roy A, Feng Y (2017) Model-based population pharmacokinetic analysis of nivolumab in patients with solid tumors. CPT Pharmacometrics Syst Pharmacol 6(1):58–66. https://doi.org/10.1002/psp4.12143

Bauer RJ, Dedrick RL, White ML, Murray MJ, Garovoy MR (1999) Population pharmacokinetics and pharmacodynamics of the anti-CD11a antibody hu1124 in human

subjects with psoriasis. J Pharmacokinet Biopharm 27(4):397–420
Baxter LT, Zhu H, Mackensen DG, Jain RK (1994) Physiologically based pharmacokinetic model for specific and nonspecific monoclonal antibodies and fragments in normal tissues and human tumor xenografts in nude mice. Cancer Res 54(6):1517–1528
Baxter LT, Zhu H, Mackensen DG, Butler WF, Jain RK (1995) Biodistribution of monoclonal antibodies: scale-up from mouse to human using a physiologically based pharmacokinetic model. Cancer Res 55(20):4611–4622
Bazin-Redureau MI, Renard CB, Scherrmann JM (1997) Pharmacokinetics of heterologous and homologous immunoglobulin G, F(ab')2 and Fab after intravenous administration in the rat. J Pharm Pharmacol 49(3):277–281
Berger MA, Masters GR, Singleton J, Scully MS, Grimm LG, Soltis DA, Albone EF (2005) Pharmacokinetics, biodistribution, and radioimmunotherapy with monoclonal antibody 776.1 in a murine model of human ovarian cancer. Cancer Biother Radiopharm 20(6):589–602
Bien-Ly N, Boswell CA, Jeet S, Beach TG, Hoyte K, Luk W, Shihadeh V, Ulufatu S, Foreman O, Lu Y, DeVoss J, van der Brug M, Watts RJ (2015) Lack of widespread BBB disruption in Alzheimer's disease models: focus on therapeutic antibodies. Neuron 88(2):289–297. https://doi.org/10.1016/j.neuron.2015.09.036
Bittner B, Richter WF, Hourcade-Potelleret F, McIntyre C, Herting F, Zepeda ML, Schmidt J (2012) Development of a subcutaneous formulation for trastuzumab - nonclinical and clinical bridging approach to the approved intravenous dosing regimen. Arzneimittelforschung 62(9):401–409. https://doi.org/10.1055/s-0032-1321831
Boswell CA, Brechbiel MW (2007) Development of radioimmunotherapeutic and diagnostic antibodies: an inside-out view. Nucl Med Biol 34(7):757–778. https://doi.org/10.1016/j.nucmedbio.2007.04.001
Boswell CA, Ferl GZ, Mundo EE, Schweiger MG, Marik J, Reich MP, Theil FP, Fielder PJ, Khawli LA (2010a) Development and evaluation of a novel method for preclinical measurement of tissue vascular volume. Mol Pharm 7(5):1848–1857. https://doi.org/10.1021/mp100183k
Boswell CA, Tesar DB, Mukhyala K, Theil FP, Fielder PJ, Khawli LA (2010b) Effects of charge on antibody tissue distribution and pharmacokinetics. Bioconjug Chem 21(12):2153–2163. https://doi.org/10.1021/bc100261d
Boswell CA, Bumbaca D, Fielder PJ, Khawli LA (2012) Compartmental tissue distribution of antibody therapeutics: experimental approaches and interpretations. AAPS J 14(3):612–618. https://doi.org/10.1208/s12248-012-9374-1
Boswell CA, Mundo EE, Johnstone B, Ulufatu S, Schweiger MG, Bumbaca D, Fielder PJ, Prabhu S, Khawli LA (2013) Vascular physiology and protein disposition in a preclinical model of neurodegeneration. Mol Pharm 10(5):1514–1521. https://doi.org/10.1021/mp3004786
Boswell CA, Mundo EE, Ulufatu S, Bumbaca D, Cahaya HS, Majidy N, Van Hoy M, Schweiger MG, Fielder PJ, Prabhu S, Khawli LA (2014) Comparative physiology of mice and rats: radiometric measurement of vascular parameters in rodent tissues. Mol Pharm 11(5):1591–1598. https://doi.org/10.1021/mp400748t
Boxenbaum H, Battle M (1995) Effective half-life in clinical pharmacology. J Clin Pharmacol 35(8):763–766
Brambell FW, Hemmings WA, Morris IG (1964) A theoretical model of gamma-globulin catabolism. Nature 203:1352–1354
Bugelski PJ, Herzyk DJ, Rehm S, Harmsen AG, Gore EV, Williams DM, Maleeff BE, Badger AM, Truneh A, O'Brien SR, Macia RA, Wier PJ, Morgan DG, Hart TK (2000) Preclinical development of keliximab, a primatized anti-CD4 monoclonal antibody, in human CD4 transgenic mice: characterization of the model and safety studies. Hum Exp Toxicol 19(4):230–243. https://doi.org/10.1191/096032700678815783
Bumbaca Yadav D, Sharma VK, Boswell CA, Hotzel I, Tesar D, Shang Y, Ying Y, Fischer SK, Grogan JL, Chiang EY, Urban K, Ulufatu S, Khawli LA, Prabhu S, Joseph S, Kelley RF (2015) Evaluating the use of antibody variable region (Fv) charge as a risk assessment tool for predicting typical cynomolgus monkey pharmacokinetics. J Biol Chem 290(50):29732–29741. https://doi.org/10.1074/jbc.M115.692434
Bumbaca D, Wong A, Drake E, Reyes AE, Lin BC, Stephan JP, Desnoyers L, Shen BQ, Dennis MS (2011) Highly specific off-target binding identified and eliminated during the humanization of an antibody against FGF receptor 4. MAbs 3(4):376–386
Bumbaca D, Xiang H, Boswell CA, Port RE, Stainton SL, Mundo EE, Ulufatu S, Bagri A, Theil FP, Fielder PJ, Khawli LA, Shen BQ (2012) Maximizing tumour exposure to anti-neuropilin-1 antibody requires saturation of non-tumour tissue antigenic sinks in mice. Br J Pharmacol 166(1):368–377. https://doi.org/10.1111/j.1476-5381.2011.01777.x
Bunescu A, Seideman P, Lenkei R, Levin K, Egberg N (2004) Enhanced Fcgamma receptor I, alphaMbeta2 integrin receptor expression by monocytes and neutrophils in rheumatoid arthritis: interaction with platelets. J Rheumatol 31(12):2347–2355
Cartron G, Watier H, Golay J, Solal-Celigny P (2004) From the bench to the bedside: ways to improve rituximab efficacy. Blood 104(9):2635–2642
CDER (2014) Clinical pharmacology and biopharmaceutical reviews BLA 125522
CDER (2015) Addendum clinical pharmacology review BLA 125509. https://www.accessdata.fda.gov/drugsatfda_docs/nda/2016/125509Orig1s000ClinPharmR.pdf. Accessed May 8, 2018
Chen Y, Samineni D, Mukadam S, Wong H, Shen BQ, Lu D, Girish S, Hop C, Jin JY, Li C (2015) Physiologically based pharmacokinetic modeling as a tool to predict drug interactions for antibody-drug conjugates. Clin Pharmacokinet 54(1):81–93. https://doi.org/10.1007/s40262-014-0182-x
Chen SC, Kagedal M, Gao Y, Wang B, Harle-Yge ML, Girish S, Jin J, Li C (2017) Population pharmacokinetics of trastuzumab emtansine in previously treated patients with HER2-positive advanced gastric cancer (AGC). Cancer

Chemother Pharmacol 80(6):1147–1159. https://doi.org/10.1007/s00280-017-3443-1

Chien JY, Friedrich S, Heathman MA, de Alwis DP, Sinha V (2005) Pharmacokinetics/pharmacodynamics and the stages of drug development: role of modeling and simulation. AAPS J 7(3):E544–E559

Clarke J, Leach W, Pippig S, Joshi A, Wu B, House R, Beyer J (2004) Evaluation of a surrogate antibody for preclinical safety testing of an anti-CD11a monoclonal antibody. Regul Toxicol Pharmacol 40(3):219–226

Coffey GP, Fox JA, Pippig S, Palmieri S, Reitz B, Gonzales M, Bakshi A, Padilla-Eagar J, Fielder PJ (2005) Tissue distribution and receptor-mediated clearance of anti-CD11a antibody in mice. Drug Metab Dispos 33(5):623–629

Cohenuram M, Saif MW (2007) Panitumumab the first fully human monoclonal antibody: from the bench to the clinic. Anti-Cancer Drugs 18(1):7–15

Cornillie F, Shealy D, D'Haens G, Geboes K, Van Assche G, Ceuppens J, Wagner C, Schaible T, Plevy SE, Targan SR, Rutgeerts P (2001) Infliximab induces potent anti-inflammatory and local immunomodulatory activity but no systemic immune suppression in patients with Crohn's disease. Aliment Pharmacol Ther 15(4):463–473

Dall'Ozzo S, Tartas S, Paintaud G, Cartron G, Colombat P, Bardos P, Watier H, Thibault G (2004) Rituximab-dependent cytotoxicity by natural killer cells: influence of FCGR3A polymorphism on the concentration-effect relationship. Cancer Res 64(13):4664–4669

Danilov SM, Gavrilyuk VD, Franke FE, Pauls K, Harshaw DW, McDonald TD, Miletich DJ, Muzykantov VR (2001) Lung uptake of antibodies to endothelial antigens: key determinants of vascular immunotargeting. Am J Physiol Lung Cell Mol Physiol 280(6):L1335–L1347

Davda JP, Dodds MG, Gibbs MA, Wisdom W, Gibbs J (2014) A model-based meta-analysis of monoclonal antibody pharmacokinetics to guide optimal first-in-human study design. MAbs 6(4):1094–1102. https://doi.org/10.4161/mabs.29095

Davis JD, Bansal A, Hassman D, Akinlade B, Li M, Li Z, Swanson B, Hamilton JD, DiCioccio AT (2018) Evaluation of potential disease-mediated drug-drug interaction in patients with moderate-to-severe atopic dermatitis receiving dupilumab. Clin Pharmacol Ther. https://doi.org/10.1002/cpt.1058

Dedrick RL (1973) Animal scale-up. J Pharmacokinet Biopharm 1(5):435–461

Deng R, Iyer S, Theil FP, Mortensen DL, Fielder PJ, Prabhu S (2011) Projecting human pharmacokinetics of therapeutic antibodies from nonclinical data: what have we learned? MAbs 3(1):61–66

Dias C, Abosaleem B, Crispino C, Gao B, Shaywitz A (2015a) Erratum to: tolerability of high-volume subcutaneous injections of a viscous placebo buffer: a randomized, crossover study in healthy subjects. AAPS PharmSciTech 16(6):1500. https://doi.org/10.1208/s12249-015-0324-y

Dias C, Abosaleem B, Crispino C, Gao B, Shaywitz A (2015b) Tolerability of high-volume subcutaneous injections of a viscous placebo buffer: a randomized, crossover study in healthy subjects. AAPS PharmSciTech 16(5):1101–1107. https://doi.org/10.1208/s12249-015-0288-y

Dickinson BL, Badizadegan K, Wu Z, Ahouse JC, Zhu X, Simister NE, Blumberg RS, Lencer WI (1999) Bidirectional FcRn-dependent IgG transport in a polarized human intestinal epithelial cell line. J Clin Invest 104(7):903–911

Dirks NL, Meibohm B (2010) Population pharmacokinetics of therapeutic monoclonal antibodies. Clin Pharmacokinet 49(10):633–659. https://doi.org/10.2165/11535960-000000000-00000

Dong JQ, Salinger DH, Endres CJ, Gibbs JP, Hsu CP, Stouch BJ, Hurh E, Gibbs MA (2011) Quantitative prediction of human pharmacokinetics for monoclonal antibodies: retrospective analysis of monkey as a single species for first-in-human prediction. Clin Pharmacokinet 50(2):131–142. https://doi.org/10.2165/11537430-000000000-00000

Dostalek M, Prueksaritanont T, Kelley RF (2017) Pharmacokinetic de-risking tools for selection of monoclonal antibody lead candidates. MAbs 9(5):756–766. https://doi.org/10.1080/19420862.2017.1323160

Dowell JA, Korth-Bradley J, Liu H, King SP, Berger MS (2001) Pharmacokinetics of gemtuzumab ozogamicin, an antibody-targeted chemotherapy agent for the treatment of patients with acute myeloid leukemia in first relapse. J Clin Pharmacol 41(11):1206–1214

Druet P, Bariety J, Laliberte F, Bellon B, Belair MF, Paing M (1978) Distribution of heterologous antiperoxidase antibodies and their fragments in the superficial renal cortex of normal Wistar-Munich rat: an ultrastructural study. Lab Investig 39(6):623–631

Duconge J, Castillo R, Crombet T, Alvarez D, Matheu J, Vecino G, Alonso K, Beausoleil I, Valenzuela C, Becquer MA, Fernandez-Sanchez E (2004) Integrated pharmacokinetic-pharmacodynamic modeling and allometric scaling for optimizing the dosage regimen of the monoclonal ior EGF/r3 antibody. Eur J Pharm Sci 21(2-3):261–270

Fasanmade AA, Adedokun OJ, Ford J, Hernandez D, Johanns J, Hu C, Davis HM, Zhou H (2009) Population pharmacokinetic analysis of infliximab in patients with ulcerative colitis. Eur J Clin Pharmacol 65(12):1211–1228. https://doi.org/10.1007/s00228-009-0718-4

Fasanmade AA, Adedokun OJ, Olson A, Strauss R, Davis HM (2010) Serum albumin concentration: a predictive factor of infliximab pharmacokinetics and clinical response in patients with ulcerative colitis. Int J Clin Pharmacol Ther 48(5):297–308

FDA (1999) Guidance for industry: population pharmacokinetics

Ferl GZ, Wu AM, DiStefano JJ (2005) A predictive model of therapeutic monoclonal antibody dynamics and regulation by the neonatal Fc receptor (FcRn). Ann Biomed Eng 33(11):1640–1652

Frost GI (2007) Recombinant human hyaluronidase (rHuPH20): an enabling platform for subcutaneous drug and fluid administration. Expert Opin Drug Deliv 4(4):427–440. https://doi.org/10.1517/17425247.4.4.427

Garg A, Quartino A, Li J, Jin J, Wada DR, Li H, Cortes J, McNally V, Ross G, Visich J, Lum B (2014) Population pharmacokinetic and covariate analysis of pertuzumab, a HER2-targeted monoclonal antibody, and evaluation of a fixed, non-weight-based dose in patients with a variety of solid tumors. Cancer Chemother Pharmacol 74(4):819–829. https://doi.org/10.1007/s00280-014-2560-3

Genovese MC, Cohen S, Moreland L, Lium D, Robbins S, Newmark R, Bekker P, Study G (2004) Combination therapy with etanercept and anakinra in the treatment of patients with rheumatoid arthritis who have been treated unsuccessfully with methotrexate. Arthritis Rheum 50(5):1412–1419. https://doi.org/10.1002/art.20221

Ghetie V, Hubbard JG, Kim JK, Tsen MF, Lee Y, Ward ES (1996) Abnormally short serum half-lives of IgG in beta 2-microglobulin-deficient mice. Eur J Immunol 26(3):690–696

Gibiansky L, Frey N (2012) Linking interleukin-6 receptor blockade with tocilizumab and its hematological effects using a modeling approach. J Pharmacokinet Pharmacodyn 39(1):5–16. https://doi.org/10.1007/s10928-011-9227-z

Gibiansky L, Gibiansky E (2009) Target-mediated drug disposition model: relationships with indirect response models and application to population PK-PD analysis. J Pharmacokinet Pharmacodyn 36(4):341–351. https://doi.org/10.1007/s10928-009-9125-9

Gibiansky L, Sutjandra L, Doshi S, Zheng J, Sohn W, Peterson MC, Jang GR, Chow AT, Perez-Ruixo JJ (2012) Population pharmacokinetic analysis of denosumab in patients with bone metastases from solid tumours. Clin Pharmacokinet 51(4):247–260. https://doi.org/10.2165/11598090-000000000-00000

Gillies SD, Lan Y, Lo KM, Super M, Wesolowski J (1999) Improving the efficacy of antibody-interleukin 2 fusion proteins by reducing their interaction with Fc receptors. Cancer Res 59(9):2159–2166

Gillies SD, Lo KM, Burger C, Lan Y, Dahl T, Wong WK (2002) Improved circulating half-life and efficacy of an antibody-interleukin 2 immunocytokine based on reduced intracellular proteolysis. Clin Cancer Res 8(1):210–216

Girish G, Li C (2015) Clinical pharmacology and assay consideration for characterizing pharmacokinetics and understanding efficacy and safety of antibody-drug conjugates. In: Gorovits B, Shord S (eds) Novel methods in bioanalysis and characterization of antibody-drug conjugate. Future Science Ltd, London, pp 36–55

Girish S, Martin SW, Peterson MC et al (2011) AAPS workshop report: strategies to address therapeutic protein–drug interactions during clinical development. APPS J 3:405–416

Goldsby RA, Kindt TJ, Osborine BA, Kuby J (1999) Immunology, 4th edn. W.H. Freeman and Company, New York

Gottlieb AB, Miller B, Lowe N, Shapiro W, Hudson C, Bright R, Ling M, Magee A, McCall CO, Rist T, Dummer W, Walicke P, Bauer RJ, White M, Garovoy M (2003) Subcutaneously administered efalizumab (anti-CD11a) improves signs and symptoms of moderate to severe plaque psoriasis. J Cutan Med Surg 7(3):198–207

Han K, Jin J, Maia M, Lowe J, Sersch MA, Allison DE (2014) Lower exposure and faster clearance of bevacizumab in gastric cancer and the impact of patient variables: analysis of individual data from AVAGAST phase III trial. AAPS J 16(5):1056–1063. https://doi.org/10.1208/s12248-014-9631-6

Hayashi N, Tsukamoto Y, Sallas WM, Lowe PJ (2007) A mechanism-based binding model for the population pharmacokinetics and pharmacodynamics of omalizumab. Br J Clin Pharmacol 63(5):548–561. https://doi.org/10.1111/j.1365-2125.2006.02803.x

Herceptin (Trastuzumab) Prescribing Information (2006) South San Francisco, CA, USA

Hervey PS, Keam SJ (2006) Abatacept. BioDrugs 20(1):53–61

Hinton PR, Xiong JM, Johlfs MG, Tang MT, Keller S, Tsurushita N (2006) An engineered human IgG1 antibody with longer serum half-life. J Immunol 176(1):346–356

Hochhaus G, Brookman L, Fox H, Johnson C, Matthews J, Ren S, Deniz Y (2003) Pharmacodynamics of omalizumab: implications for optimised dosing strategies and clinical efficacy in the treatment of allergic asthma. Curr Med Res Opin 19(6):491–498. https://doi.org/10.1185/030079903125002171

Holmes D (2011) Buy buy bispecific antibodies. Nat Rev Drug Discov 10(11):798–800. https://doi.org/10.1038/nrd3581

Honma W, Gautier A, Paule I, Yamaguchi M, Lowe PJ (2016) Ethnic sensitivity assessment of pharmacokinetics and pharmacodynamics of omalizumab with dosing table expansion. Drug Metab Pharmacokinet 31(3):173–184. https://doi.org/10.1016/j.dmpk.2015.12.003

Hooks MA, Wade CS, Millikan WJ Jr (1991) Muromonab CD-3: a review of its pharmacology, pharmacokinetics, and clinical use in transplantation. Pharmacotherapy 11(1):26–37

Huang SM, Zhao H, Lee JI, Reynolds K, Zhang L, Temple R, Lesko LJ (2010) Therapeutic protein-drug interactions and implications for drug development. Clin Pharmacol Ther 87(4):497–503. https://doi.org/10.1038/clpt.2009.308

Humira (Adalimumab) Prescribing Information (2007) Chicago, IL, USA

ICH (1997a) ICH harmonized tripartite guideline M3: nonclinical safety studies for the conduct of human clinical trials for pharmaceuticals

ICH (1997b) ICH harmonized tripartite guideline S6: preclinical safety evaluation of biotechnology-derived pharmaceuticals

Igawa T, Tsunoda H, Tachibana T, Maeda A, Mimoto F, Moriyama C, Nanami M, Sekimori Y, Nabuchi Y, Aso Y, Hattori K (2010) Reduced elimination of IgG antibodies by engineering the variable region. Protein Eng Des Sel 23(5):385–392. https://doi.org/10.1093/protein/gzq009

Jolling K, Perez Ruixo JJ, Hemeryck A, Vermeulen A, Greway T (2005) Mixed-effects modelling of the interspecies

pharmacokinetic scaling of pegylated human erythropoietin. Eur J Pharm Sci 24(5):465–475

Joshi A, Bauer R, Kuebler P, White M, Leddy C, Compton P, Garovoy M, Kwon P, Walicke P, Dedrick R (2006) An overview of the pharmacokinetics and pharmacodynamics of efalizumab: a monoclonal antibody approved for use in psoriasis. J Clin Pharmacol 46(1):10–20

Junghans RP (1997) Finally! The Brambell receptor (FcRB). Mediator of transmission of immunity and protection from catabolism for IgG. Immunol Res 16(1):29–57

Junghans RP, Anderson CL (1996) The protection receptor for IgG catabolism is the beta2-microglobulin-containing neonatal intestinal transport receptor. Proc Natl Acad Sci U S A 93(11):5512–5516

Kagan L, Abraham AK, Harrold JM, Mager DE (2010) Interspecies scaling of receptor-mediated pharmacokinetics and pharmacodynamics of type I interferons. Pharm Res 27(5):920–932. https://doi.org/10.1007/s11095-010-0098-6

Kagedal M, Gibiansky L, Xu J, Wang X, Samineni D, Chen SC, Lu D, Agarwal P, Wang B, Saad O, Koppada N, Fine BM, Jin JY, Girish S, Li C (2017) Platform model describing pharmacokinetic properties of vc-MMAE antibody-drug conjugates. J Pharmacokinet Pharmacodyn 44(6):537–548. https://doi.org/10.1007/s10928-017-9544-y

Kairemo KJ, Lappalainen AK, Kaapa E, Laitinen OM, Hyytinen T, Karonen SL, Gronblad M (2001) In vivo detection of intervertebral disk injury using a radiolabeled monoclonal antibody against keratan sulfate. J Nucl Med 42(3):476–482

Kamath AV (2016) Translational pharmacokinetics and pharmacodynamics of monoclonal antibodies. Drug Discov Today Technol 21-22:75–83. https://doi.org/10.1016/j.ddtec.2016.09.004

Kang YK, Ryu MH, Yoo C, Ryoo BY, Kim HJ, Lee JJ, Nam BH, Ramaiya N, Jagannathan J, Demetri GD (2013) Resumption of imatinib to control metastatic or unresectable gastrointestinal stromal tumours after failure of imatinib and sunitinib (RIGHT): a randomised, placebo-controlled, phase 3 trial. Lancet Oncol 14(12):1175–1182. https://doi.org/10.1016/S1470-2045(13)70453-4

Kelley SK, Gelzleichter T, Xie D, Lee WP, Darbonne WC, Qureshi F, Kissler K, Oflazoglu E, Grewal IS (2006) Preclinical pharmacokinetics, pharmacodynamics, and activity of a humanized anti-CD40 antibody (SGN-40) in rodents and non-human primates. Br J Pharmacol 148(8):1116–1123

Kenny JR, Liu MM, Chow AT, Earp JC, Evers R, Slatter JG, Wang DD, Zhang L, Zhou H (2013) Therapeutic protein drug-drug interactions: navigating the knowledge gaps-highlights from the 2012 AAPS NBC roundtable and IQ consortium/FDA workshop. AAPS J 15(4):933–940. https://doi.org/10.1208/s12248-013-9495-1

Khawli LA, Goswami S, Hutchinson R, Kwong ZW, Yang J, Wang X, Yao Z, Sreedhara A, Cano T, Tesar D, Nijem I, Allison DE, Wong PY, Kao YH, Quan C, Joshi A, Harris RJ, Motchnik P (2010) Charge variants in IgG1: isolation, characterization, in vitro binding properties and pharmacokinetics in rats. MAbs 2(6):613–624. https://doi.org/10.4161/mabs.2.6.13333

Kirschbrown WP, Quartino AL, Li H, Mangat R, Wada DR, Garg A, Jin JY, Lum BL (2017) Development of a population pharmacokinetic (PPK) model of intravenous (IV) trastuzumab in patients with a variety of solid tumors to support dosing and treatment recommendations. J Clin Oncol 35(Suppl):2525

Kleiman NS, Raizner AE, Jordan R, Wang AL, Norton D, Mace KF, Joshi A, Coller BS, Weisman HF (1995) Differential inhibition of platelet aggregation induced by adenosine diphosphate or a thrombin receptor-activating peptide in patients treated with bolus chimeric 7E3 Fab: implications for inhibition of the internal pool of GPIIb/IIIa receptors. J Am Coll Cardiol 26(7):1665–1671. https://doi.org/10.1016/0735-1097(95)00391-6

Kohler G, Milstein C (1975) Continuous cultures of fused cells secreting antibody of predefined specificity. Nature 256(5517):495–497

Kolar GR, Capra JD (2003) Immunoglobulins: structure and function. In: Paul WE (ed) Fundamental immunology, 5th edn. Lippincott Williams & Wilkins, Philadelphia

Koon HB, Severy P, Hagg DS, Butler K, Hill T, Jones AG, Waldmann TA, Junghans RP (2006) Antileukemic effect of daclizumab in CD25 high-expressing leukemias and impact of tumor burden on antibody dosing. Leuk Res 30(2):190–203

Kovalenko P, DiCioccio AT, Davis JD, Li M, Ardeleanu M, Graham N, Soltys R (2016) Exploratory population PK analysis of dupilumab, a fully human monoclonal antibody against IL-4ralpha, in atopic dermatitis patients and normal volunteers. CPT Pharmacometrics Syst Pharmacol 5(11):617–624. https://doi.org/10.1002/psp4.12136

Kovarik JM, Nashan B, Neuhaus P, Clavien PA, Gerbeau C, Hall ML, Korn A (2001) A population pharmacokinetic screen to identify demographic-clinical covariates of basiliximab in liver transplantation. Clin Pharmacol Ther 69(4):201–209

Krueger JG (2002) The immunologic basis for the treatment of psoriasis with new biologic agents. J Am Acad Dermatol 46(1):1–23

Kuus-Reichel K, Grauer LS, Karavodin LM, Knott C, Krusemeier M, Kay NE (1994) Will immunogenicity limit the use, efficacy, and future development of therapeutic monoclonal antibodies? Clin Diagn Lab Immunol 1(4):365–372

Lee H, Kimko HC, Rogge M, Wang D, Nestorov I, Peck CC (2003) Population pharmacokinetic and pharmacodynamic modeling of etanercept using logistic regression analysis. Clin Pharmacol Ther 73(4):348–365

Lee JI, Zhang L, Men AY, Kenna LA, Huang SM (2010) CYP-mediated therapeutic protein-drug interactions: clinical findings, proposed mechanisms and regulatory implications. Clin Pharmacokinet 49(5):295–310. https://doi.org/10.2165/11319980-000000000-00000

Li B, Tesar D, Boswell CA, Cahaya HS, Wong A, Zhang J, Meng YG, Eigenbrot C, Pantua H, Diao J, Kapadia SB, Deng R, Kelley RF (2014) Framework selection can influence pharmacokinetics of a humanized therapeutic

antibody through differences in molecule charge. MAbs 6(5):1255–1264. https://doi.org/10.4161/mabs.29809

Li H, Yu J, Liu C, Liu J, Subramaniam S, Zhao H, Blumenthal GM, Turner DC, Li C, Ahamadi M, de Greef R, Chatterjee M, Kondic AG, Stone JA, Booth BP, Keegan P, Rahman A, Wang Y (2017) Time dependent pharmacokinetics of pembrolizumab in patients with solid tumor and its correlation with best overall response. J Pharmacokinet Pharmacodyn 44(5):403–414. https://doi.org/10.1007/s10928-017-9528-y

Lin YS, Nguyen C, Mendoza JL, Escandon E, Fei D, Meng YG, Modi NB (1999) Preclinical pharmacokinetics, interspecies scaling, and tissue distribution of a humanized monoclonal antibody against vascular endothelial growth factor. J Pharmacol Exp Ther 288(1):371–378

Ling J, Zhou H, Jiao Q, Davis HM (2009) Interspecies scaling of therapeutic monoclonal antibodies: initial look. J Clin Pharmacol 49(12):1382–1402. https://doi.org/10.1177/0091270009337134

Liu J, Wang Y, Zhao L (2015) Assessment of exposure-response (E-R) and cse-control (C-C) analyses in oncology using simulation based approach. In: Am Conf. Pharmacometrics Ann Meeting

Lobo ED, Hansen RJ, Balthasar JP (2004) Antibody pharmacokinetics and pharmacodynamics. J Pharm Sci 93(11):2645–2668

Looney RJ, Anolik JH, Campbell D, Felgar RE, Young F, Arend LJ, Sloand JA, Rosenblatt J, Sanz I (2004) B cell depletion as a novel treatment for systemic lupus erythematosus: a phase I/II dose-escalation trial of rituximab. Arthritis Rheum 50(8):2580–2589

LoRusso PM, Weiss D, Guardino E, Girish S, Sliwkowski MX (2011) Trastuzumab emtansine: a unique antibody-drug conjugate in development for human epidermal growth factor receptor 2-positive cancer. Clin Cancer Res 17(20):6437–6447. https://doi.org/10.1158/1078-0432.CCR-11-0762

Lowe PJ, Georgiou P, Canvin J (2015) Revision of omalizumab dosing table for dosing every 4 instead of 2 weeks for specific ranges of bodyweight and baseline IgE. Regul Toxicol Pharmacol 71(1):68–77. https://doi.org/10.1016/j.yrtph.2014.12.002

Lu D, Burris HA, Wang B, Dees EC, Cortes J, Joshi A, Gupta M, Yi JH, Chu YW, Shih T, Fang L, Girish S (2012) Drug interaction potential of trastuzumab emtansine (T-DM1) combined with pertuzumab in patients with HER2-positive metastatic breast cancer. Curr Drug Metab 13(7):911–922

Lu D, Girish S, Gao Y, Wang B, Yi JH, Guardino E, Samant M, Cobleigh M, Rimawi M, Conte P, Jin JY (2014) Population pharmacokinetics of trastuzumab emtansine (T-DM1), a HER2-targeted antibody-drug conjugate, in patients with HER2-positive metastatic breast cancer: clinical implications of the effect of covariates. Cancer Chemother Pharmacol 74(2):399–410. https://doi.org/10.1007/s00280-014-2500-2

Ma P, Yang BB, Wang YM, Peterson M, Narayanan A, Sutjandra L, Rodriguez R, Chow A (2009) Population pharmacokinetic analysis of panitumumab in patients with advanced solid tumors. J Clin Pharmacol 49(10):1142–1156. https://doi.org/10.1177/0091270009344989

Mager DE, Mascelli MA, Kleiman NS, Fitzgerald DJ, Abernethy DR (2003) Simultaneous modeling of abciximab plasma concentrations and ex vivo pharmacodynamics in patients undergoing coronary angioplasty. J Pharmacol Exp Ther 307(3):969–976. https://doi.org/10.1124/jpet.103.057299

Mager DE, Woo S, Jusko WJ (2009) Scaling pharmacodynamics from in vitro and preclinical animal studies to humans. Drug Metab Pharmacokinet 24(1):16–24

Mahmood I (2005) Prediction of concentration-time profiles in humans. Pine House Publisher, Rockville

Mahmood I (2009) Pharmacokinetic allometric scaling of antibodies: application to the first-in-human dose estimation. J Pharm Sci 98(10):3850–3861. https://doi.org/10.1002/jps.21682

Mahmood I, Green MD (2005) Pharmacokinetic and pharmacodynamic considerations in the development of therapeutic proteins. Clin Pharmacokinet 44(4):331–347

Maini RN, Breedveld FC, Kalden JR, Smolen JS, Davis D, Macfarlane JD, Antoni C, Leeb B, Elliott MJ, Woody JN, Schaible TF, Feldmann M (1998) Therapeutic efficacy of multiple intravenous infusions of anti-tumor necrosis factor alpha monoclonal antibody combined with low-dose weekly methotrexate in rheumatoid arthritis. Arthritis Rheum 41(9):1552–1563. https://doi.org/10.1002/1529-0131(199809)41:9<1552::AID-ART5>3.0.CO;2-W

Mandikian D, Takahashi N, Lo AA, Li J, Eastham-Anderson J, Slaga D, Ho J, Hristopoulos M, Clark R, Totpal K, Lin K, Joseph SB, Dennis MS, Prabhu S, Junttila TT, Boswell CA (2018) Relative target affinities of T-cell-dependent bispecific antibodies determine biodistribution in a solid tumor mouse model. Mol Cancer Ther 17(4):776–785. https://doi.org/10.1158/1535-7163.MCT-17-0657

Martin-Jimenez T, Riviere JE (2002) Mixed-effects modeling of the interspecies pharmacokinetic scaling of oxytetracycline. J Pharm Sci 91(2):331–341

McClurkan MB, Valentine JL, Arnold L, Owens SM (1993) Disposition of a monoclonal anti-phencyclidine Fab fragment of immunoglobulin G in rats. J Pharmacol Exp Ther 266(3):1439–1445

McLaughlin P, Grillo-Lopez AJ, Link BK, Levy R, Czuczman MS, Williams ME, Heyman MR, Bence-Bruckler I, White CA, Cabanillas F, Jain V, Ho AD, Lister J, Wey K, Shen D, Dallaire BK (1998) Rituximab chimeric anti-CD20 monoclonal antibody therapy for relapsed indolent lymphoma: half of patients respond to a four-dose treatment program. J Clin Oncol 16(8):2825–2833

Medesan C, Matesoi D, Radu C, Ghetie V, Ward ES (1997) Delineation of the amino acid residues involved in transcytosis and catabolism of mouse IgG1. J Immunol 158(5):2211–2217

Meibohm B, Derendorf H (2002) Pharmacokinetic/pharmacodynamic studies in drug product development. J Pharm Sci 91(1):18–31

Meijer RT, Koopmans RP, ten Berge IJ, Schellekens PT (2002) Pharmacokinetics of murine anti-human CD3

antibodies in man are determined by the disappearance of target antigen. J Pharmacol Exp Ther 300(1): 346–353

Meredith PA, Elliott HL, Donnelly R, Reid JL (1991) Dose-response clarification in early drug development. J Hypertens Suppl 9(6):S356–S357

Morris EC, Rebello P, Thomson KJ, Peggs KS, Kyriakou C, Goldstone AH, Mackinnon S, Hale G (2003) Pharmacokinetics of alemtuzumab used for in vivo and in vitro T-cell depletion in allogeneic transplantations: relevance for early adoptive immunotherapy and infectious complications. Blood 102(1):404–406. https://doi.org/10.1182/blood-2002-09-2687

Mortensen DL, Walicke PA, Wang X, Kwon P, Kuebler P, Gottlieb AB, Krueger JG, Leonardi C, Miller B, Joshi A (2005) Pharmacokinetics and pharmacodynamics of multiple weekly subcutaneous efalizumab doses in patients with plaque psoriasis. J Clin Pharmacol 45(3):286–298

Mould DR, Sweeney KR (2007) The pharmacokinetics and pharmacodynamics of monoclonal antibodies--mechanistic modeling applied to drug development. Curr Opin Drug Discov Devel 10(1):84–96

Mould DR, Davis CB, Minthorn EA, Kwok DC, Elliott MJ, Luggen ME, Totoritis MC (1999) A population pharmacokinetic-pharmacodynamic analysis of single doses of clenoliximab in patients with rheumatoid arthritis. Clin Pharmacol Ther 66(3):246–257

den Broeder A, van de Putte L, Rau R, Schattenkirchner M, Van Riel P, Sander O, Binder C, Fenner H, Bankmann Y, Velagapudi R, Kempeni J, Kupper H (2002) A single dose, placebo controlled study of the fully human anti-tumor necrosis factor-alpha antibody adalimumab (D2E7) in patients with rheumatoid arthritis. J Rheumatol 29(11):2288–2298

Nakakura EK, McCabe SM, Zheng B, Shorthouse RA, Scheiner TM, Blank G, Jardieu PM, Morris RE (1993) Potent and effective prolongation by anti-LFA-1 monoclonal antibody monotherapy of non-primarily vascularized heart allograft survival in mice without T cell depletion. Transplantation 55(2):412–417

Nestorov I, Zitnik R, Ludden T (2004) Population pharmacokinetic modeling of subcutaneously administered etanercept in patients with psoriasis. J Pharmacokinet Pharmacodyn 31(6):463–490

Ng CM, Joshi A, Dedrick RL, Garovoy MR, Bauer RJ (2005) Pharmacokinetic-pharmacodynamic-efficacy analysis of efalizumab in patients with moderate to severe psoriasis. Pharm Res 22(7):1088–1100

Ng CM, Stefanich E, Anand BS, Fielder PJ, Vaickus L (2006) Pharmacokinetics/pharmacodynamics of nondepleting anti-CD4 monoclonal antibody (TRX1) in healthy human volunteers. Pharm Res 23(1):95–103

Norman DJ, Chatenoud L, Cohen D, Goldman M, Shield CF 3rd (1993) Consensus statement regarding OKT3-induced cytokine-release syndrome and human anti-mouse antibodies. Transplant Proc 25(2 Suppl 1):89–92

Ober RJ, Radu CG, Ghetie V, Ward ES (2001) Differences in promiscuity for antibody-FcRn interactions across species: implications for therapeutic antibodies. Int Immunol 13(12):1551–1559

Oitate M, Masubuchi N, Ito T, Yabe Y, Karibe T, Aoki T, Murayama N, Kurihara A, Okudaira N, Izumi T (2011) Prediction of human pharmacokinetics of therapeutic monoclonal antibodies from simple allometry of monkey data. Drug Metab Pharmacokinet 26(4): 423–430

Page MM, Watts GF (2015) Evolocumab in the treatment of dyslipidemia: pre-clinical and clinical pharmacology. Expert Opin Drug Metab Toxicol 11(9):1505–1515. https://doi.org/10.1517/17425255.2015.1073712

Papp K, Bissonnette R, Krueger JG, Carey W, Gratton D, Gulliver WP, Lui H, Lynde CW, Magee A, Minier D, Ouellet JP, Patel P, Shapiro J, Shear NH, Kramer S, Walicke P, Bauer R, Dedrick RL, Kim SS, White M, Garovoy MR (2001) The treatment of moderate to severe psoriasis with a new anti-CD11a monoclonal antibody. J Am Acad Dermatol 45(5):665–674

Petkova SB, Akilesh S, Sproule TJ, Christianson GJ, Al Khabbaz H, Brown AC, Presta LG, Meng YG, Roopenian DC (2006) Enhanced half-life of genetically engineered human IgG1 antibodies in a humanized FcRn mouse model: potential application in humorally mediated autoimmune disease. Int Immunol 18(12):1759–1769

Prabhu S, Boswell CA, Leipold D, Khawli LA, Li D, Lu D, Theil FP, Joshi A, Lum BL (2011) Antibody delivery of drugs and radionuclides: factors influencing clinical pharmacology. Ther Deliv 2(6):769–791

Presta LG (2002) Engineering antibodies for therapy. Curr Pharm Biotechnol 3(3):237–256

Presta LG, Shields RL, Namenuk AK, Hong K, Meng YG (2002) Engineering therapeutic antibodies for improved function. Biochem Soc Trans 30(4):487–490

Putnam WS, Prabhu S, Zheng Y, Subramanyam M, Wang YM (2010) Pharmacokinetic, pharmacodynamic and immunogenicity comparability assessment strategies for monoclonal antibodies. Trends Biotechnol 28(10):509–516. https://doi.org/10.1016/j.tibtech.2010.07.001

Raptiva (Efalizumab) [Prescribing Information] (2004) South San Francisco, Calif: Genentech, Inc

Roopenian DC, Christianson GJ, Sproule TJ, Brown AC, Akilesh S, Jung N, Petkova S, Avanessian L, Choi EY, Shaffer DJ, Eden PA, Anderson CL (2003) The MHC class I-like IgG receptor controls perinatal IgG transport, IgG homeostasis, and fate of IgG-Fc-coupled drugs. J Immunol 170(7):3528–3533

Roskos LK, Davis CG, Schwab GM (2004) The clinical pharmacology of therapeutic monoclonal antibodies. Drug Dev Res 61:108–120

Ryman JT, Meibohm B (2017) Pharmacokinetics of monoclonal antibodies. CPT Pharmacometrics Syst Pharmacol 6(9):576–588. https://doi.org/10.1002/psp4.12224

Sampei Z, Igawa T, Soeda T, Okuyama-Nishida Y, Moriyama C, Wakabayashi T, Tanaka E, Muto A, Kojima T, Kitazawa T, Yoshihashi K, Harada A, Funaki M, Haraya K, Tachibana T, Suzuki S, Esaki K, Nabuchi Y, Hattori K (2013) Identification and multidimensional optimization of an asymmetric bispecific IgG antibody

mimicking the function of factor VIII cofactor activity. PLoS One 8(2):e57479. https://doi.org/10.1371/journal.pone.0057479

Schmitt C, Kuhn B, Zhang X, Kivitz AJ, Grange S (2011) Disease-drug-drug interaction involving tocilizumab and simvastatin in patients with rheumatoid arthritis. Clin Pharmacol Ther 89(5):735–740. https://doi.org/10.1038/clpt.2011.35

Schror K, Weber AA (2003) Comparative pharmacology of GP IIb/IIIa antagonists. J Thromb Thrombolysis 15(2):71–80

Shah DK, Betts AM (2012) Towards a platform PBPK model to characterize the plasma and tissue disposition of monoclonal antibodies in preclinical species and human. J Pharmacokinet Pharmacodyn 39(1):67–86. https://doi.org/10.1007/s10928-011-9232-2

Sheiner LB (1997) Learning versus confirming in clinical drug development. Clin Pharmacol Ther 61(3):275–291

Sheiner L, Wakefield J (1999) Population modelling in drug development. Stat Methods Med Res 8(3):183–193

Shields RL, Namenuk AK, Hong K, Meng YG, Rae J, Briggs J, Xie D, Lai J, Stadlen A, Li B, Fox JA, Presta LG (2001) High resolution mapping of the binding site on human IgG1 for Fc gamma RI, Fc gamma RII, Fc gamma RIII, and FcRn and design of IgG1 variants with improved binding to the Fc gamma R. J Biol Chem 276(9):6591–6604

Sifontis NM, Benedetti E, Vasquez EM (2002) Clinically significant drug interaction between basiliximab and tacrolimus in renal transplant recipients. Transplant Proc 34(5):1730–1732

Simister NE, Mostov KE (1989a) Cloning and expression of the neonatal rat intestinal Fc receptor, a major histocompatibility complex class I antigen homolog. Cold Spring Harb Symp Quant Biol 54(Pt 1):571–580

Simister NE, Mostov KE (1989b) An Fc receptor structurally related to MHC class I antigens. Nature 337(6203):184–187

Simulect (Basiliximab) Prescribing Information (2005) East Hanover, NJ, USA

Slatter JG, Wienkers LC, Dickmann LC (2013) Drug interactions of cytokines and anticytokine therapeutic proteins. Drug-drug interactions for therapeutics biologics. Wiley, Hoboken

Spiekermann GM, Finn PW, Ward ES, Dumont J, Dickinson BL, Blumberg RS, Lencer WI (2002) Receptor-mediated immunoglobulin G transport across mucosal barriers in adult life: functional expression of FcRn in the mammalian lung. J Exp Med 196(3):303–310

Straughn JM, Oliver PG, Zhou T, Wang W, Alvarez RD, Grizzle WE, Buchsbaum DJ (2006) Anti-tumor activity of TRA-8 anti-death receptor 5 (DR5) monoclonal antibody in combination with chemotherapy and radiation therapy in a cervical cancer model. Gynecol Oncol 101(1):46–54. https://doi.org/10.1016/j.ygyno.2005.09.053

Struemper H, Sale M, Patel BR, Ostergaard M, Osterborg A, Wierda WG, Hagenbeek A, Coiffier B, Jewell RC (2014) Population pharmacokinetics of ofatumumab in patients with chronic lymphocytic leukemia, follicular lymphoma, and rheumatoid arthritis. J Clin Pharmacol 54(7):818–827. https://doi.org/10.1002/jcph.268

Subramanian GM, Cronin PW, Poley G, Weinstein A, Stoughton SM, Zhong J, Ou Y, Zmuda JF, Osborn BL, Freimuth WW (2005) A phase 1 study of PAmAb, a fully human monoclonal antibody against Bacillus anthracis protective antigen, in healthy volunteers. Clin Infect Dis 41(1):12–20

Sun YN, Lu JF, Joshi A, Compton P, Kwon P, Bruno RA (2005) Population pharmacokinetics of efalizumab (humanized monoclonal anti-CD11a antibody) following long-term subcutaneous weekly dosing in psoriasis subjects. J Clin Pharmacol 45(4):468–476

Tabrizi MA, Tseng CM, Roskos LK (2006) Elimination mechanisms of therapeutic monoclonal antibodies. Drug Discov Today 11(1-2):81–88

Tang H, Mayersohn M (2005) Accuracy of allometrically predicted pharmacokinetic parameters in humans: role of species selection. Drug Metab Dispos 33(9):1288–1293

Tang L, Persky AM, Hochhaus G, Meibohm B (2004) Pharmacokinetic aspects of biotechnology products. J Pharm Sci 93(9):2184–2204. https://doi.org/10.1002/jps.20125

Ternant D, Paintaud G (2005) Pharmacokinetics and concentration-effect relationships of therapeutic monoclonal antibodies and fusion proteins. Expert Opin Biol Ther 5(Suppl 1):S37–S47

Thurber GM, Schmidt MM, Wittrup KD (2008) Antibody tumor penetration: transport opposed by systemic and antigen-mediated clearance. Adv Drug Deliv Rev 60(12):1421–1434. https://doi.org/10.1016/j.addr.2008.04.012

Tran JQ, Othman AA, Wolstencroft P, Elkins J (2016) Therapeutic protein-drug interaction assessment for daclizumab high-yield process in patients with multiple sclerosis using a cocktail approach. Br J Clin Pharmacol 82(1):160–167. https://doi.org/10.1111/bcp.12936

Trianni.com (2018) http://trianni.com/technology/mouse/. Accessed May 8, 2018

Umana P, Jean-Mairet J, Moudry R, Amstutz H, Bailey JE (1999) Engineered glycoforms of an antineuroblastoma IgG1 with optimized antibody-dependent cellular cytotoxic activity. Nat Biotechnol 17(2):176–180

Vaccaro C, Bawdon R, Wanjie S, Ober RJ, Ward ES (2006) Divergent activities of an engineered antibody in murine and human systems have implications for therapeutic antibodies. Proc Natl Acad Sci U S A 103(49):18709–18714

Vaishnaw AK, TenHoor CN (2002) Pharmacokinetics, biologic activity, and tolerability of alefacept by intravenous and intramuscular administration. J Pharmacokinet Pharmacodyn 29(5-6):415–426

Vasquez EM, Pollak R (1997) OKT3 therapy increases cyclosporine blood levels. Clin Transpl 11(1):38–41

Vectibix (Panitumumab) Prescribing Information (2015) Thousand Oaks, CA, USA

Vincenti F, Mendez R, Pescovitz M, Rajagopalan PR, Wilkinson AH, Butt K, Laskow D, Slakey DP, Lorber MI, Garg JP, Garovoy M (2007) A phase I/II

randomized open-label multicenter trial of efalizumab, a humanized anti-CD11a, anti-LFA-1 in renal transplantation. Am J Transplant 7(7):1770–1777. https://doi.org/10.1111/j.1600-6143.2007.01845.x

Vugmeyster Y, Guay H, Szklut P, Qian MD, Jin M, Widom A, Spaulding V, Bennett F, Lowe L, Andreyeva T, Lowe D, Lane S, Thom G, Valge-Archer V, Gill D, Young D, Bloom L (2010) In vitro potency, pharmacokinetic profiles, and pharmacological activity of optimized anti-IL-21R antibodies in a mouse model of lupus. MAbs 2(3):335–346

Vugmeyster Y, Szklut P, Wensel D, Ross J, Xu X, Awwad M, Gill D, Tchistiakov L, Warner G (2011) Complex pharmacokinetics of a humanized antibody against human amyloid beta peptide, anti-abeta Ab2, in nonclinical species. Pharm Res 28(7):1696–1706. https://doi.org/10.1007/s11095-011-0405-x

Wang Y (2016) Special considerations for modeling exposure response for biologics. In: Am Soc Clin Pharmacol and Therapeutics Ann Meeting

Wang W, Prueksaritanont T (2010) Prediction of human clearance of therapeutic proteins: simple allometric scaling method revisited. Biopharm Drug Dispos 31(4):253–263. https://doi.org/10.1002/bdd.708

Wang W, Singh S, Zeng DL, King K, Nema S (2007) Antibody structure, instability, and formulation. J Pharm Sci 96(1):1–26

Watanabe N, Kuriyama H, Sone H, Neda H, Yamauchi N, Maeda M, Niitsu Y (1988) Continuous internalization of tumor necrosis factor receptors in a human myosarcoma cell line. J Biol Chem 263(21):10262–10266

Weiner LM (2006) Fully human therapeutic monoclonal antibodies. J Immunother 29(1):1–9

Weiskopf K, Weissman IL (2015) Macrophages are critical effectors of antibody therapies for cancer. MAbs 7(2):303–310. https://doi.org/10.1080/19420862.2015.1011450

Weisman MH, Moreland LW, Furst DE, Weinblatt ME, Keystone EC, Paulus HE, Teoh LS, Velagapudi RB, Noertersheuser PA, Granneman GR, Fischkoff SA, Chartash EK (2003) Efficacy, pharmacokinetic, and safety assessment of adalimumab, a fully human anti-tumor necrosis factor-alpha monoclonal antibody, in adults with rheumatoid arthritis receiving concomitant methotrexate: a pilot study. Clin Ther 25(6):1700–1721

Werther WA, Gonzalez TN, O'Connor SJ, McCabe S, Chan B, Hotaling T, Champe M, Fox JA, Jardieu PM, Berman PW, Presta LG (1996) Humanization of an anti-lymphocyte function-associated antigen (LFA)-1 monoclonal antibody and reengineering of the humanized antibody for binding to rhesus LFA-1. J Immunol 157(11):4986–4995

Wiseman GA, White CA, Sparks RB, Erwin WD, Podoloff DA, Lamonica D, Bartlett NL, Parker JA, Dunn WL, Spies SM, Belanger R, Witzig TE, Leigh BR (2001) Biodistribution and dosimetry results from a phase III prospectively randomized controlled trial of Zevalin radioimmunotherapy for low-grade, follicular, or transformed B-cell non-Hodgkin's lymphoma. Crit Rev Oncol Hematol 39(1-2):181–194

Wu H, Pfarr DS, Johnson S, Brewah YA, Woods RM, Patel NK, White WI, Young JF, Kiener PA (2007) Development of motavizumab, an ultra-potent antibody for the prevention of respiratory syncytial virus infection in the upper and lower respiratory tract. J Mol Biol 368(3):652–665. https://doi.org/10.1016/j.jmb.2007.02.024

Wurster U, Haas J (1994) Passage of intravenous immunoglobulin and interaction with the CNS. J Neurol Neurosurg Psychiatry 57(Suppl):21–25

Xolair (Omalizumab) Prescribing Information (2006) South San Francisco, CA, USA & East Hanover, NJ, USA

Yadav DB, Maloney JA, Wildsmith KR, Fuji RN, Meilandt WJ, Solanoy H, Lu Y, Peng K, Wilson B, Chan P, Gadkar K, Kosky A, Goo M, Daugherty A, Couch JA, Keene T, Hayes K, Nikolas LJ, Lane D, Switzer R, Adams E, Watts RJ, Scearce-Levie K, Prabhu S, Shafer L, Thakker DR, Hildebrand K, Atwal JK (2017) Widespread brain distribution and activity following i.c.v. infusion of anti-beta-secretase (BACE1) in nonhuman primates. Br J Pharmacol 174(22):4173–4185. https://doi.org/10.1111/bph.14021

Yang J, Zhao H, Garnett C, Rahman A, Gobburu JV, Pierce W, Schechter G, Summers J, Keegan P, Booth B, Wang Y (2013) The combination of exposure-response and case-control analyses in regulatory decision making. J Clin Pharmacol 53(2):160–166. https://doi.org/10.1177/0091270012445206

Yim DS, Zhou H, Buckwalter M, Nestorov I, Peck CC, Lee H (2005) Population pharmacokinetic analysis and simulation of the time-concentration profile of etanercept in pediatric patients with juvenile rheumatoid arthritis. J Clin Pharmacol 45(3):246–256. https://doi.org/10.1177/0091270004271945

Yip V, Palma E, Tesar DB, Mundo EE, Bumbaca D, Torres EK, Reyes NA, Shen BQ, Fielder PJ, Prabhu S, Khawli LA, Boswell CA (2014) Quantitative cumulative biodistribution of antibodies in mice: effect of modulating binding affinity to the neonatal Fc receptor. MAbs 6(3):689–696. https://doi.org/10.4161/mabs.28254

Younes A, Bartlett NL, Leonard JP, Kennedy DA, Lynch CM, Sievers EL, Forero-Torres A (2010) Brentuximab vedotin (SGN-35) for relapsed CD30-positive lymphomas. N Engl J Med 363(19):1812–1821. https://doi.org/10.1056/NEJMoa1002965

Yu YJ, Atwal JK, Zhang Y, Tong RK, Wildsmith KR, Tan C, Bien-Ly N, Hersom M, Maloney JA, Meilandt WJ, Bumbaca D, Gadkar K, Hoyte K, Luk W, Lu Y, Ernst JA, Scearce-Levie K, Couch JA, Dennis MS, Watts RJ (2014) Therapeutic bispecific antibodies cross the blood-brain barrier in nonhuman primates. Sci Transl Med 6(261):261ra154. https://doi.org/10.1126/scitranslmed.3009835

Zenapax (Daclizumab) Prescribing Information (2005) Nutley, NJ, USA

Zheng Y, Scheerens H, Davis JC Jr, Deng R, Fischer SK, Woods C, Fielder PJ, Stefanich EG (2011) Translational pharmacokinetics and pharmacodynamics of an FcRn-variant anti-CD4 monoclonal antibody from preclinical model to phase I study. Clin Pharmacol Ther 89(2):283–290. https://doi.org/10.1038/clpt.2010.311

Zhou H (2005) Clinical pharmacokinetics of etanercept: a fully humanized soluble recombinant tumor necrosis factor receptor fusion protein. J Clin Pharmacol 45(5):490–497

Zhou H, Mayer PR, Wajdula J, Fatenejad S (2004) Unaltered etanercept pharmacokinetics with concurrent methotrexate in patients with rheumatoid arthritis. J Clin Pharmacol 44(11):1235–1243. https://doi.org/10.1177/0091270004268049

Zhu Y, Hu C, Lu M, Liao S, Marini JC, Yohrling J, Yeilding N, Davis HM, Zhou H (2009) Population pharmacokinetic modeling of ustekinumab, a human monoclonal antibody targeting IL-12/23p40, in patients with moderate to severe plaque psoriasis. J Clin Pharmacol 49(2):162–175. https://doi.org/10.1177/0091270008329556

Zhuang Y, de Vries DE, Xu Z, Marciniak SJ Jr, Chen D, Leon F, Davis HM, Zhou H (2015) Evaluation of disease-mediated therapeutic protein-drug interactions between an anti-interleukin-6 monoclonal antibody (sirukumab) and cytochrome P450 activities in a phase 1 study in patients with rheumatoid arthritis using a cocktail approach. J Clin Pharmacol 55(12):1386–1394. https://doi.org/10.1002/jcph.561

Zia-Amirhosseini P, Minthorn E, Benincosa LJ, Hart TK, Hottenstein CS, Tobia LA, Davis CB (1999) Pharmacokinetics and pharmacodynamics of SB-240563, a humanized monoclonal antibody directed to human interleukin-5, in monkeys. J Pharmacol Exp Ther 291(3):1060–1067